POLITECNICO DI TORINO

Department of Mechanical and Aerospace Engineering

Master Degree Course in Aerospace Engineering

Master's Thesis

Development of an Electrical Power System for a 3U educational CubeSat

Supervisors
Prof. Fabrizio Stesina
Prof. Sabrina Corpino

Candidate
Emanuela La Bella

December 2022

To knowledge and scientific progress

Abstract

The CubeSats world is in continuous expansion, thanks to their low cost, fast delivery and easy implementation, which make them affordable for all interested stakeholders in space research and universities. The Politecnico di Torino has a great history behind the development of educational CubeSats, which continues today with the study of an Earth observation mission in Low Earth Orbit (LEO). This mission is called SILVA (Satellite-based Innovative Land and Vegetation Analysis) and is being carried out by a student team, the CubeSat Team, within which the work of this thesis is located.

The main objective of the thesis is the development of an Electrical Power System (EPS), which plays a key role in the success of a space mission, as it is responsible for the management of the power generation, the storage of the energy and its distribution to all subsystems of the small satellite. The EPS developed in the thesis finds application in the 3U CubeSat of SILVA mission.

This thesis focuses on the study of a dependable design of the EPS, starting with an overview of the state of the art and continuing with an advanced functional analysis of the subsystem in order to identify its requirements. As a consequence, the study of a preliminary configuration has been performed, as well as the analysis of the power required by the other subsystems of the CubeSat. Finally, these analysis results in the overall sizing of the EPS, which required several iterations due to the close interaction with the design evolution of the other subsystems. The EPS development continues with the manufacturing of its hardware components (solar panels, batteries, power management board), that includes an initial phase of components identification in accordance with the proposed design, and a subsequent phase consisting in the procurement of the identified hardware solutions. The thesis goes on with the elaboration of an Assembly, Integration and Verification (AIV) plan, the study of the EPS performances, through analysis performed with the MATLAB software, and the verification of part of the requirements identified in the first design phase, through the use of instrumentations and test benches available in the Systems and Technologies for Aerospace Research laboratory (STARlab) of the Department of Mechanical and Aerospace Engineering (DIMEAS) of the Politecnico di Torino.

The development of the Electrical Power System and the results obtained in this thesis are intended as a useful reference for both future enhancements of the EPS of the SILVA CubeSat and the work of EPS developers for different CubeSat missions around the world.

Table of Contents

List of figures

List of tables

Acronyms

A	Ampere
ADC	Analog to Digital Converter
ADCS	Attitude Determination and Control System
Ah	Ampere-hour
AIV	Assembly Integration and Verification
BCR	Battery Charge Regulator
BOL	Beginning Of Life
BMS	Battery Management System
CAN	Controller Area Network
CC	Constant Current
CDS	CubeSat Design Specification
CESI	Centro Elettrotecnico Sperimentale Italiano
cm	centimeter
ComSys	Communication System
ConOps	Concept of Operations
COTS	Commercial Off The Shelf
CP	Cal Poly
CTJ-LC	Cell Triple Junction - Low Cost
CV	Constant Voltage
DC	Direct Current
DIMEAS	Department of Mechanical and Aerospace Engineering
DOD	Depth Of Discharge
E-st@r-I	Educational SaTellite @ politecnico di toRino I
E-st@r-II	Educational SaTellite @ politecnico di toRino II
EFM	Electrical and Functional Model
EOL	End Of Life
EOP	Early Orbit Phase
EPS	Electrical Power System
ESA	European Space Agency
ESD	Electrostatic Discharge
FBD	Functional Block Diagram
FE	Function/Equipment
FFBD	Functional Flow Block Diagram
FM	Flight Model
g	gram
G	Gain
GaAs	Gallium Arsenide
Ge	Germanium

GSE	Ground Support Equipment
h	hour
hPa	Hectopascal
I2C	Inter Integrated Circuit
I_{mp}	Current at Maximum Power
I_{sc}	Short Circuit Current
InGaP	Indium Gallium Phosphide
ISO	International Organization for Standardization
ISS	International Space Station
LCL	Latching Current Limiter
LEOP	Launch and Early Orbit Phase
Li-ion	Lithium-ion
LiPo	Lithium Polymer
mA	milliAmpere
MCU	MicroController Unit
min	minutes
MPP	Maximum Power Point
MPPT	Maximum Power Point Tracker
mW	milliWatt
NASA	National Aeronautics and Space Administration
NiCd	Nickel-Cadmium
NiH2	Nickel-Hydrogen
NRCSD	NanoRacks CubeSat Deployer
NTC	Negative Temperature Coefficient
OBC	On Board Computer
Op amp	Operational Amplifier
P_{max}	Maximum Power
PBD	Physical Block Diagram
PC	Personal Computer
PCDU	Power Conditioning and Distribution Unit
PCU	Power Conditioning Unit
PDU	Power Distribution Unit
RBF	Remove Before Flight
RGB	Red Green Blue
RS-232	Recommended Standard 232
SEPIC	Single Ended Primary Inductor Converter
SILVA	Satellite-based Innovative Land and Vegetation Analysis
SOC	State Of Charge
SPI	Serial Peripheral Interface
SRR	Super-Resolution Reconstruction
SSO	Sun-Synchronous Orbit

STARlab	Systems and Technologies for Aerospace Research laboratory
TBD	To Be Determined
TCS	Thermal Control System
U	Unit
UHF	Ultra High Frequency
USB	Universal Serial Bus
V	Volt
V_{mp}	Voltage at Maximum Power
V_{oc}	Open Circuit Voltage
VMU	Virtual Mock-Up
W	Watt
Wh	Watt-hour
µC	MicroController
µm	Micron
Ω	Ohm
@	at
°	Degree
°C	Degree Celsius
3S2P	3 Series/2 Parallel

1 Introduction

The Earth is constantly changing slowly in a natural way and more rapidly because of human activities. The need to observe the Earth from space derives from necessities in several fields, such as clouds, oceans and atmosphere monitoring in meteorology, the study of land, crop and vegetation characteristics in agriculture and forestry, monitoring of environmental pollution, sand and dust storms, fires, snow cover in disaster management and even ice mapping and ocean color monitoring in cartography.

Artificial objects as small satellites have been developed to meet these needs, orbiting around the Earth or another planet. They are smaller, lighter, faster, and more affordable than conventional satellites and can do even more, as small satellites are able to perform missions that a larger satellite could not, such as academic research, testing and/or qualification of new hardware, in-orbit inspection of larger satellites, the utilisation of swarms to collect data from multiple points and constellations for low data rate communication.

A Small Satellite is a miniaturised satellite with a weight of no more than 180 kg, and it is classified according to its mass in the following categories [1]:

- Minisatellites (100-180 kg);
- Microsatellites (10-100 kg);
- Nanosatellites (1-10 kg);
- Picosatellites (0.01 – 1 kg).

The Nanosatellites category includes CubeSats, a class of satellites that adopt a standard size of one unit or 1U, representing a 10 cm cubic shape with a mass not greater than 2 kg per unit. This shape is extendable to larger sizes such as 1.5U, 2U, 3U, 6U and 12U. The 6U and 12U CubeSats fall into the Microsatellites category due to their mass, although it is common to use the term Nanosat to identify a CubeSat. The CubeSat family is shown in Figure 1.1.

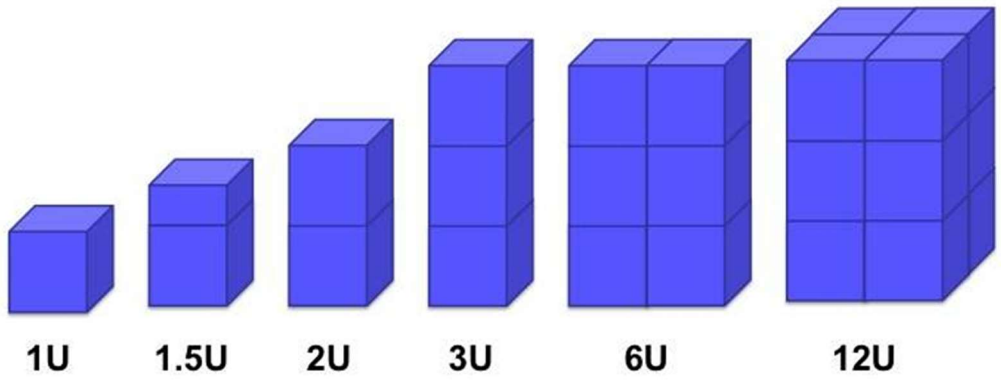

Figure 1.1: *CubeSat family. Credit: NASA [1]*

In 1999, a collaboration between Professor Jordi Puig-Suari at California Polytechnic State University (Cal Poly), San Luis Obispo, and Professor Bob Twiggs at Stanford University's Space Systems Development Laboratory (SSDL), resulting in the design of a small educational platform, the first CubeSat, for space exploration with academic purposes, simplifying access for university students and researchers due to the considerable costs and development time reductions, and the possibility of supporting frequent launches through the available launch opportunities in most of the launch vehicles.

Figure 1.2: *CP1 (Cal Poly 1) CubeSat. Credit: PolySat [2]*

This collaboration led to the definition of the CubeSat standard, defined by the CubeSat Design Specification (CDS) to which every CubeSat must be compliant in order to be launched in orbit. Indeed, the CubeSat standard is intended to provide CubeSat design specifications ranging from 1U to 12U, and to provide information on available CubeSat dispensers and their corresponding interfaces [3], encouraging the development of a highly modular and integrated system that allows the use of Commercial Off The Shelf (COTS) subsystems. The adoption of the CubeSat standard by not only universities and research institutes, but also by private companies and governmental organisations, has led to increased interest in CubeSats worldwide for scientific purposes and technology demonstrations, resulting in 1897[1] CubeSats being developed around the world and successfully launched into orbit.

The current philosophy on space exploration democritises the development of cheaper satellites in a shorter time frame and make it accessible to all kinds of companies, including universities. For example, Italian univerisities benefit from that philosophy and in Turin in particular, the Politecnico di Torino can boast the excellence of having launched two CubeSats: E-st@r-I and E-st@r-II, that were entirely developed by a university student group born in 2008, known as the CubeSat Team. In 2012, the first Italian CubeSat launched into orbit during Vega launch vehicle's maiden flight was E-st@r-I, a 1U CubeSat whose primary objective was the demonstration of an active ADCS technology, based on inertial and magnetic measurements, and its secondary objective was the testing of COTS components

[1] Facts as of 2022 August 1 [24]

and materials in space environment [4]. After just four year, in 2016, the 1U E-st@r-II was launched as part of the first edition of ESA *Fly Your Satellite!* Programme, aiming at a hands-on experience-based educational objective and technology demonstration objectives, concerning the demonstration of the autonomous attitude determination and control capability of an active ADCS technology and the in-orbit testing of COTS subsystems and in-house developed hardware and software [5].

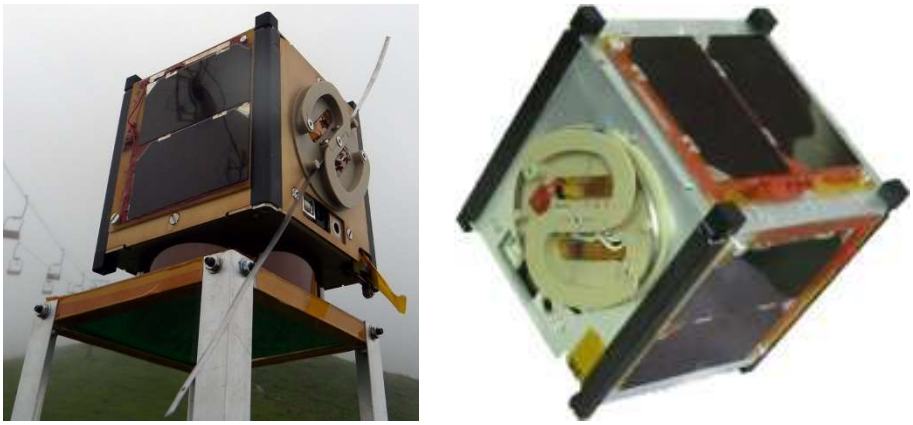

Figure 1.3: *E-st@r-I (left) and E-st@r-II (right) CubeSats. Credit: Politecnico di Torino*

This thesis work has been carried out as part of the CubeSat Team new Earth observation mission development: SILVA (Satellite-based Innovative Land and Vegetation Analysis) is a 3U educational CubeSat, that accommodate an optical payload to study the hydration status of vegetation. Indeed, the mission aims to contribute to the mitigation of climate change's effects by the application of low-cost remote sensing technology. The scientific objectives of SILVA are:

- Identify and analyse the effects of climate change on large green areas by mapping specific areas and comparing the acquired data over time;
- Collect data about the health and hydration status of vegetation, which can be used to prevent desertification and to evaluate the effectiveness of restoration measures in degraded areas;
- Identify the presence of water bodies in the vicinity of the above areas and assess their changes over the duration of the mission.

To achieve these objectives, an RGB camera is required to provide a mapping of the interested areas, by collecting images and performing on-board data processing. The technology demonstration objectives concern the testing of a Super-Resolution Reconstruction (SRR) algorithm, which would increase the quality of the available data, and the testing of the dependable approach adopted in the CubeSat design, which would show the ability to recover from many failures by reconfiguring itself and distributing its functions among the on-board processors [6].

The purpose of this thesis is the study of the Electrical Power System (EPS) of the SILVA CubeSat, that could be adopted in a similar way for the EPS design of a generical 3U educational CubeSat. In more detail, this thesis will address the design development starting with the functional analysis, the power budget definition and the subsequent system sizing, continuing with the requirements definition, the system manufacturing and the Assembly, Integration and Verification (AIV) plan activities setup, and concluding with the requirements verification through simulation analyses and functional and performance tests. Therefore, the main goal of the thesis is to develop and verify the capabilities of the EPS. But a valid question may arise at this point.

What is the EPS? It is an essential CubeSat subsystem, which ensures the survival and proper operation of the Cubesat itself, by providing power to the payload and other subsystems, such as the Attitude Determination and Control System (ADCS), the Communication System (ComSys) and the On Board Computer (OBC), and for these reasons must be dependable.

As the state of the art stands [1], a typical EPS has a centralised architecture and is made of solar cells, batteries and a Power Conditioning and Distribution Unit (PCDU), which respectively deal with the generation, storage and distribution of the power.
Solar cells are made of semiconductor layers, which use a physical and chemical phenomenon, known as the photovoltaic effect, to convert the sunlight in electric current. An old solution was the single-junction cells, that have a tradition in low-cost but also low efficiency (less than 20%). On the other hand, multi-junction solar cells are widely used in modern time, because their multiple thin layers (3 to 5 junctions) provide higher efficiencies up to 32%. However, the most challenging limitations of solar cells are their high surface area, no power generation during eclipse periods, the degradation due to aging and radiation absorption during the entire mission and the lower effectiveness in deep-space missions. The most promising solutions under development include advanced multi-junction, flexible and organic solar cells. In the first category, several four-junction solar cell architectures are currently achieving an efficiency of 38% under laboratory conditions, while five and six-junction cells with a theoretical efficiency of 70% have been experimented. Flexible solar cells are also lightweight and low-cost, as they have a layer as thin as 1 μm compared to conventional solar cell layers of 350 μm, and they can potentially be employed in deep space applications. Organic solar cells use organic electronics, in particular conductive organic polymers or small organic molecules, which absorb a large amount of sunlight and are lightweight, flexible and cheap.
Batteries are necessary for on-board power storage, which is mainly required during eclipse periods or peak loads. They are classified into primary batteries, which are not rechargeable and are used for short missions, and secondary batteries, which are the most widely used because they are rechargeable, have low weight and high energy. In the past, Nickel-Cadmium (NiCd) and Nickel-Hydrogen (NiH2) secondary batteries were used extensively on small satellites, while today, Lithium-ion (Li-ion) or Lithium Polymer (LiPo) secondary batteries are preferred. Nevertheless, repeated charging cycles cause Li-ion batteries

degradation, which results in a reduction of the energy that can be provided. For this reason, Li-ion batteries are subjected to life tests under mission conditions before being launched into orbit. Nowadays, the efforts to improve storage capability and energy density, and to increase safety by reducing the risks of combustion due to physical damage and thermal runaway due to overcharges, lead to the development of supercapacitors, Li-ion capacitors and solid-state batteries. Supercapacitors are capable of withstanding rapid charge/discharge cycles, offer very high power density, useful for transient power demands, and also can contribute to weight reduction. The Li-ion capacitor is an excellent compromise between energy density and power density, combining the energy storage capabilities of both Li-ion batteries and capacitors. On the other hand, solid-state batteries are under experimentation and may achieve considerably more energy than current Li-ion batteries, while also ensuring the elimination of the risk of combustion and capacity loss over time.
PCDU distributes power to all subsystems and instruments of the satellite and is also involved in conditioning the power in other words, mitigating possible transient disturbances and fault conditions from spreading back and causing damage to the connected loads. This allows the electronics and batteries to be protected from off-nominal conditions. The centralised architecture ensures simplicity, volume efficiency and affordable costs, but its limitation consists of non-adaptability to different missions. In order not to design every mission from scratch, a standardisation on PCDU is necessary. However, wireless sensing and power transmission technology (from microwatts up to kilowatts) exists and may be useful as a redundant option in the event of physical connectors contamination due to dusty environments, or if a hardware, such as batteries, needs to be swapped and powered.

An overview about solar cells, solar panels, batteries and PCDUs for 3U CubeSats from available manufacturers is presented in Table A - 1, Table A - 2, Table A - 3 and Table A - 4, respectively, in Appendix A.

2 Electrical Power System design

The EPS is one of the most important subsystems in all kinds of satellites and plays a responsible role in the success of the satellite's operations, since it provides power to the satellite during its operational life. To better focus on the scenario in which the EPS should operate, a mission overview is introduced in Section 2.1. The next step is the identification of the EPS functional architecture, illustrated in Section 2.2, which provides a starting point for the physical architecture study.

2.1 Mission Overview

The SILVA mission objectives are governed by the CubeSat systems, that are classified in the payload system and the bus systems, usually named as subsystems. Thus, the satellite is composed by:

- Payload, that consists of an RGB camera for low-cost remote sensing, and some processing algorithms;
- ADCS, that allows the attitude of the spacecraft to be determined and controlled;
- ComSys, that provides communications to/from ground;
- OBC, that manages on-board operations and distributes commands among the various subsystems, while also collecting telemetry produced by the spacecraft;
- EPS, that provides, stores, distributes, and controls spacecraft electrical power;
- TCS, that meets the temperature requirements of each system, through a passive control strategy;
- Mechanisms, that deploy the deployable UHF antenna of the ComSys;
- Structure, that hosts all previous systems.

Many of these systems are dependent on the EPS for their operation. To better understand the operations to be performed by SILVA CubeSat, the mission phases are shown in the Table 2.1. Further descriptions of the mission scenarios for each sub-phase are given in the Table B - 1 in Appendix B.

Mission Phase	Mission Sub-phase	Duration
LEOP	Launch	~ 90 minutes
	Deployment ConOps1	Seconds
	Deployment ConOps2	
	EOP	10 days
Operative Phase	Science Operations	At least 6 months
	Technology Demonstration	
End of Life	Disposal	Under 25 years

Table 2.1: *SILVA Mission Phases*

In the Launch and Early Orbit Phase (LEOP), two different deployment sub-phase have been evaluated, because of different Concept of Operations (ConOps):

- ConOps1 assumes that the CubeSat is deployed from a launch vehicle (e.g. Vega), planned to reach a Sun-synchronous orbit (SSO) between 400 km and 700 km altitude;
- ConOps2 assumes that the CubeSat is released from the ISS, through the Nanoracks CubeSat Deployer (NRCSD), into a circular orbit with an altitude of 400 km and an inclination of 51.6°.

Therefore, it is clear that the ConOps choice affects the altitude and inclination of the satellite's orbit. In this regard, considerations on the orbital parameters to be used for the EPS sizing are addressed in Section 2.5.1.

2.2 Functional Analysis

The EPS functional analysis is carried out to identify the functions that fulfil the mission objectives and ensure the satellite is able to operate in orbit. Firstly, a functional tree has been used as a decomposition tool to identify the functions that the EPS must perform in order to guarantee the satellite's operability. The main function and the lower-level functions of the EPS have been identified by applying the How-Why methodology, consisting of a top-down approach to the question "How?" and a bottom-up one to the question "Why?". The implementation of this method is clearly visible in the functional tree shown in Figure 2.1. The EPS functions are introduced below.

1. To manage the electrical loads
    1.1. To generate the power
        1.1.1. To use a source of energy available in space
    1.2. To store the power
        1.2.1. To charge the energy storage
    1.3. To distribute the power
        1.3.1. To connect components
        1.3.2. To electrically protect the loads
    1.4. To control the power
        1.4.1. To convert the power
        1.4.2. To condition the power

Power generation must come from an energy source available in space, which is none other than the sun. The storage of the power collected from the sun is essential for the satellite's operations during eclipse periods and must be done by recharging an energy storage unit within the satellite. The distribution of the power to satellite loads takes place both through the electrical connection of the subsystem components and through

the protection of the electrical circuits against failures. Also, the power is controlled through conversion and conditioning to ensure the desired power distribution.

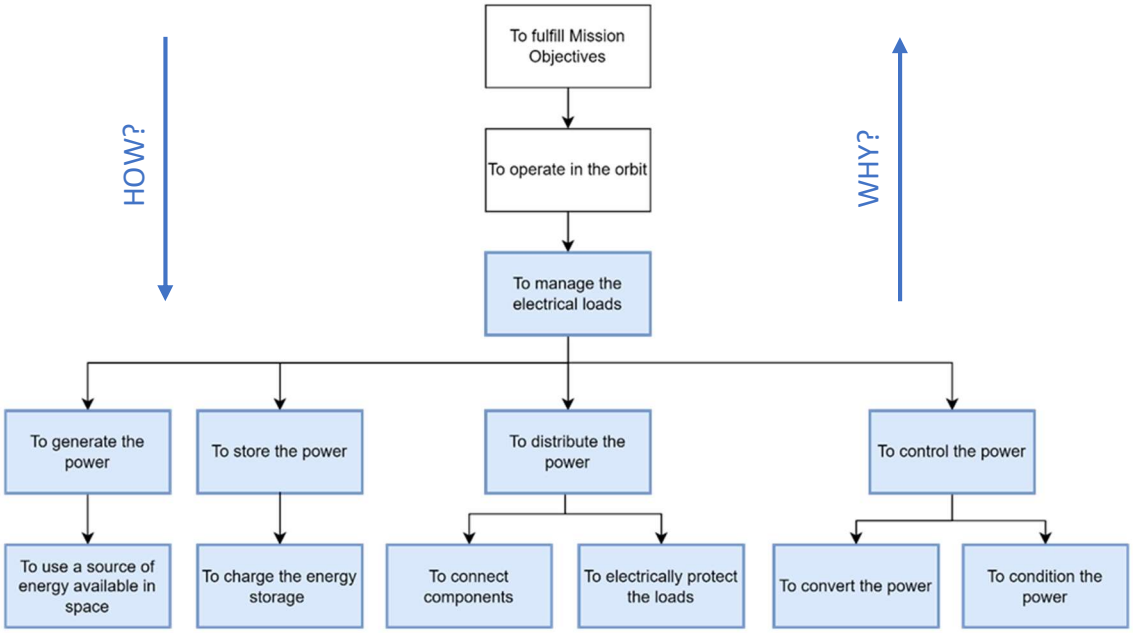

Figure 2.1: *EPS Functional Tree*

In order to analyse the time steps to be taken by the EPS, a functional flow block diagram (FFBD) has been performed. First, the EPS must obtain power from the sun. In the next steps, the EPS manages the power and charges the energy store at the same time. Next, the EPS distributes the power to the payload and each spacecraft subsystem which, at the same time, are electrically protected. Finally, the EPS sends data to the OBC.

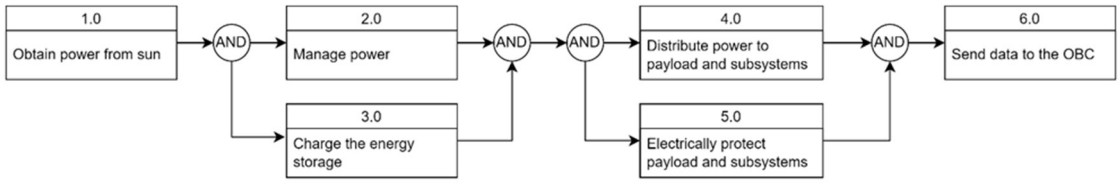

Figure 2.2: *EPS Functional Flow Block Diagram (FFBD)*

As shown in Figure 2.3, the step number 2.0 has been expanded into a second-level diagram consisting of three steps: the EPS must convert the power at the voltage required by the payload and each subsystem of the spacecraft, the EPS must regulate the power, and finally, the EPS must condition the power. Furthermore, the step number 3.0 has been expanded into two steps of the second-level diagram: the EPS fills the energy storage with power, and the EPS acquires power from the energy storage. Lastly, the step number 5.0 has been decomposed into two steps of the second-level diagram: the EPS must measure voltage, current and temperature, and the EPS must take action to cut off the payload and/or subsystems in failure.

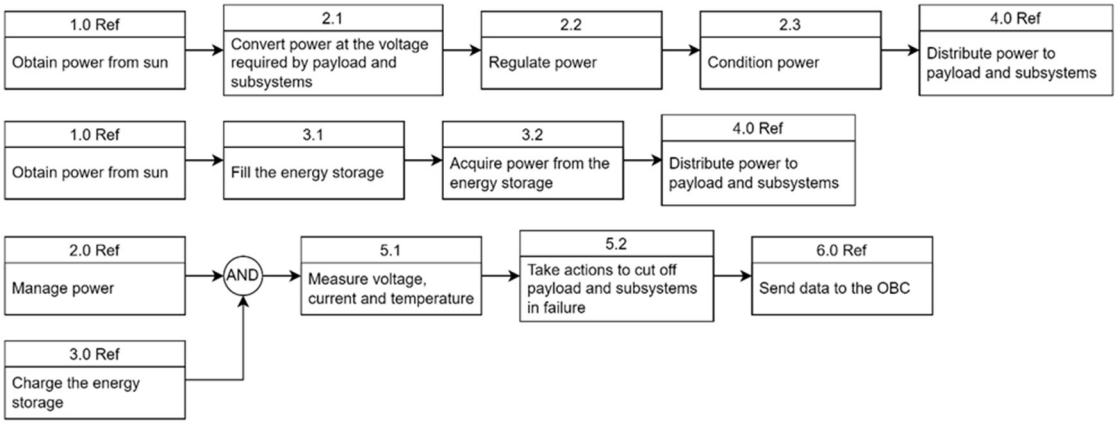

Figure 2.3: *EPS second-level FFBD*

To make a preliminary study of the physical architecture and highlight the relationships between the EPS components, the first tool implemented has been the functional block diagram (FBD). The solar panels are connected to the temperature sensors through a physical interface and to the Power Conditioning Unit (PCU) through an electrical interface. The implementation of a Maximum Power Point Tracker (MPPT) has been chosen for power regulation and conditioning. The Power Distribution Unit (PDU) consists of voltage converters and Latching Current Limiters (LCLs) for circuit protection, which allow an electrical interface with the payload and subsystems of the satellite. Between the PCU and the PDU there must be a connection to the battery pack, to enable its charging and discharging. In addition, the solar panels and batteries are both equipped with temperature sensors, so they will be connected to a Micro Controller Unit (MCU) via a data interface, which will communicate with the OBC by means of a data bus.

The EPS functional block diagram is shown in Figure 2.4, where the electrical interfaces are indicated as orange connections and the data interfaces as blue ones.

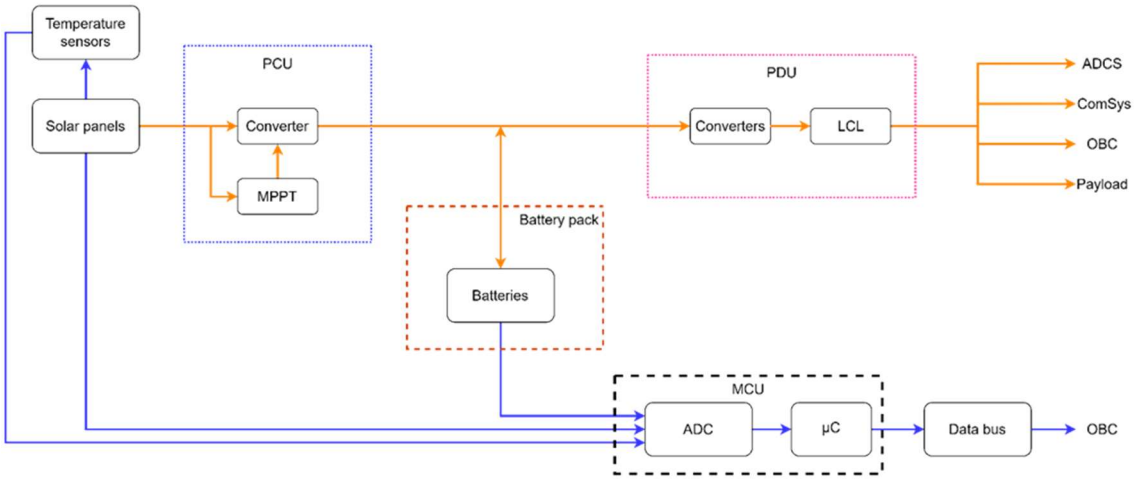

Figure 2.4: *EPS Functional Block Diagram (FBD)*

In order to correlate the functional architecture with the physical architecture, a function/equipment (FE) matrix has been performed as a verification tool for the functional analysis performed so far. The FE matrix presents the EPS functions associated with the equipment that fulfils them, and is shown in Table 2.2.

Function \ ***Equipment***	***Solar panels***	***Battery pack***	***PCDU***	***MCU***	***Power bus***
To generate the power					
To use a source of energy available in space	X				
To store the power					
To charge the energy storage		X			
To distribute the power					
To connect components					X
To electrically protect the loads			X	X	
To control the power					
To convert the power			X		
To condition the power			X		

Table 2.2: *EPS Function/Equipment matrix*

One more functional analysis tool is the N-squared diagram, implemented in order to identify the electrical/functional and mechanical/physical interfaces, and the supplied services between EPS and the other satellite systems. This tool supported the definition of the interface requirements listed in Section 2.6.

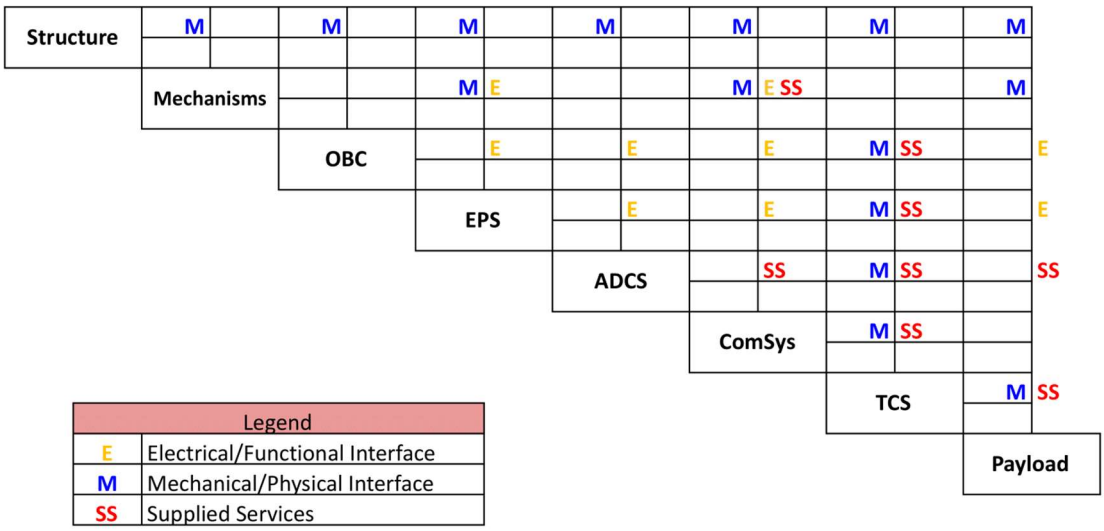

Figure 2.5: *N-squared diagram*

To finalise the functional analysis performed until here and to verify its completeness, a component-level product tree has been developed. The Figure 2.6 shows the EPS equipment and its components, which are shaded in blue.

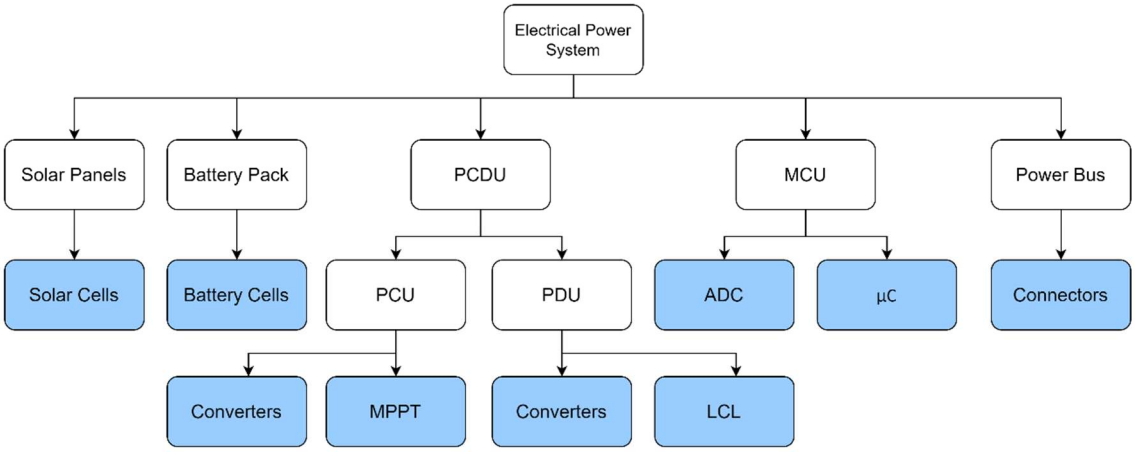

Figure 2.6: *EPS Product Tree*

2.3 Preliminary Configuration

Taking into account the available configurations on the market, a preliminary EPS configuration has been chosen in accordance with the functional analysis performed.

The body-mounted solar panels solution has been identified because of the easy implementation compared to deployable solar panels: each side face of the satellite, specifically the *x+*, *x-*, *y+* and *y-* faces, is composed of 6 solar cells as shown in Figure 2.7.

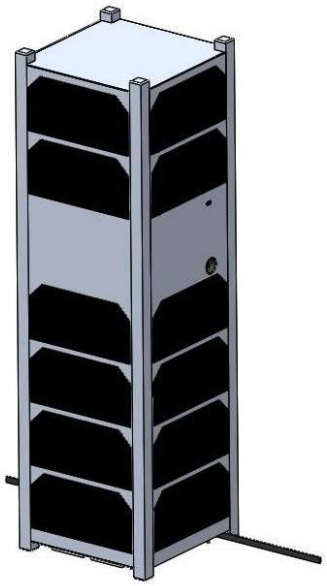

Figure 2.7: *x+ and y+ side faces and z+ upper face of the SILVA CubeSat*

Hence, a total of 24 solar cells located on the side faces of the satellite has been considered for sizing purposes. In addition, since the upper face (*z+*) has been left empty, two more solar cells may cover it, and this possibility may be considered for future developments of the configuration.

The power generated by the solar panels on opposite faces of the satellite (*x+*/*x-* and *y+*/*y-* faces) is managed by the following elements:

- 2 SEPIC converters;
- 2 MPPTs.

Each SEPIC converter and MPPT have been considered in the PCU to control the power on the opposite pair of solar panels.

The SEPIC is a DC/DC converter that provides an output voltage greater than, less than or equal to the input voltage. It is similar to a conventional buck-boost converter, but its output has the same electrical polarity as the input, which is its major advantage over a buck-boost converter. Instead, MPPT is a system that maximises power extraction from solar panels by detecting the Maximum Power Point (MPP) of the I-V curve, and thus optimising the amount of power provided to the load. It also prevents brown-outs (voltage drops) occurring when the load absorbs too much power than the solar panels are able to supply.

During sunlight, solar panels provide power directly to the satellite loads while the battery are charged when the switch that connects the solar arrays to the battery is closed. Furthermore, a protection diode is considered to prevent reverse current to the solar panels. On the other hand, during eclipse periods the power is taken from the battery pack, which is connected to the satellite loads via a switch that allows the battery to be discharged when closed. Both switches are closed when the satellite is released from the dispenser, enabling the electrical circuits to be activated as a consequence of the release of the deployment switches to which they are connected, located on the outside of the satellite structure.

The power distribution is handled by the PDU, which makes use of the four power supply lines considered:

- 3.3 V bus, dedicated to the supply of the payload, the ADCS, the ComSys and the OBC;
- 5 V bus, dedicated to supplying the payload, the ADCS and the OBC;
- 12 V bus, dedicated to the supply of the ComSys;
- Unregulated battery voltage bus.

By means of the power supply lines, the PDU ensures power distribution to the payload and all the satellite's subsystems. However, each line requires a different power

conversion and line protection, which is guaranteed by the following components provided:

- 4 buck-boost converters;
- 9 LCLs, that provide line protection from overcurrent, undervoltage and short circuits.

A buck-boost converter is a DC/DC inverting converter that provides an output voltage greater or lower than the input voltage, but its output polarity is opposite to the input one. The overcurrent, undervoltage and short circuits phenomena are detected by the LCLs and are monitored by telemetry data. In the unfortunate event that the telemetry data detect an outgoing current level unsuitable for the receiving load, or an undervoltage or short circuit, the LCLs receive an open switch command from the OBC through a microcontroller located on the PCDU board, in order to prevent the current flow from reaching the load involved.

The physical block diagram (PBD) of the preliminary configuration is shown in Figure 2.8.

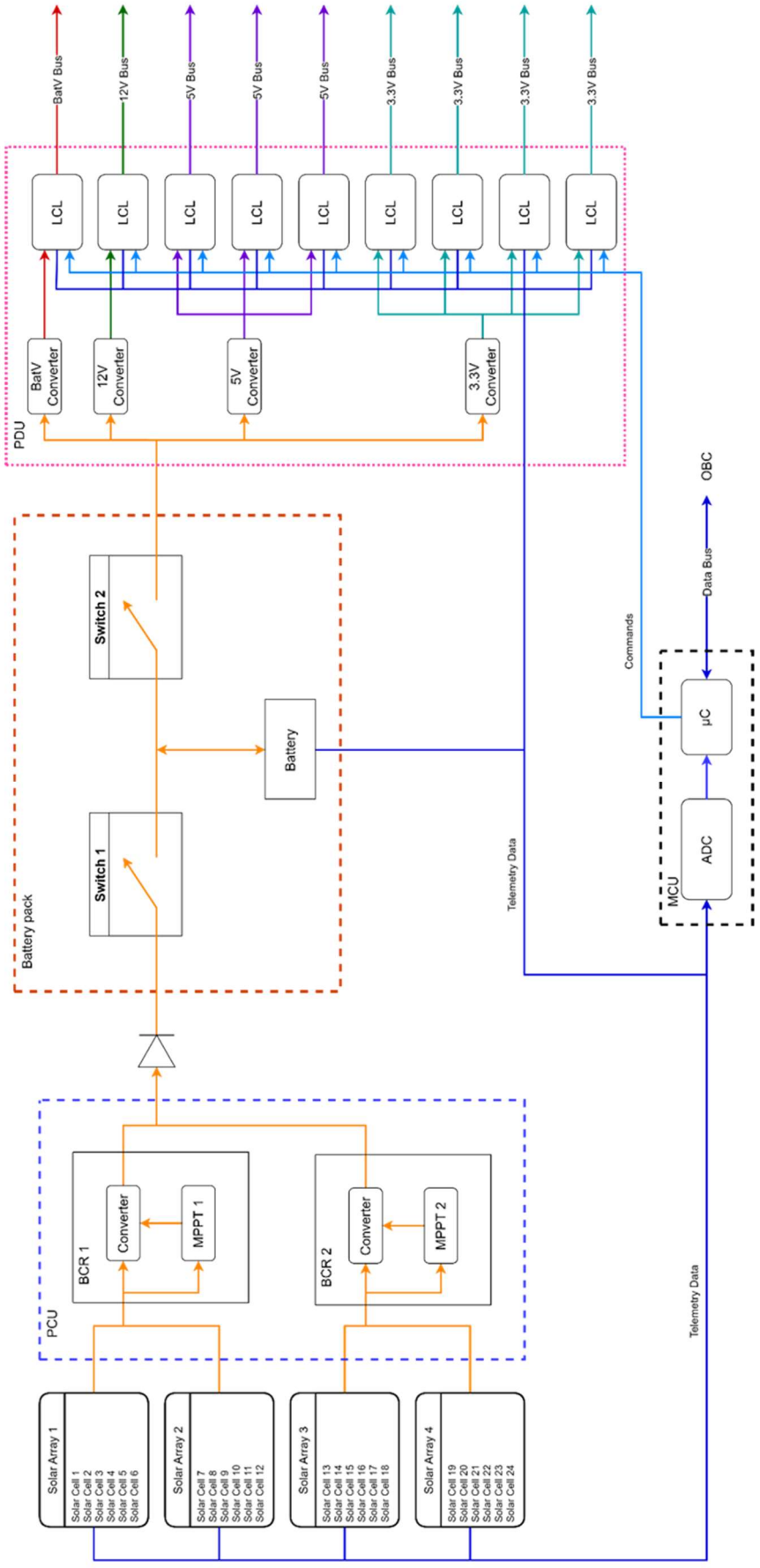

Figure 2.8: *EPS Physical Block Diagram*

2.4 Power Budget

The power budget consists of power utilisation and consumption calculation and depicts the net power balance of the satellite during its operational life. It also has a significant impact on the control and minimisation of the power demand in order to ensure consistency between power demand and power supply.

The calculations in this section and in Section 2.5 have been implemented in Matlab software as a script, reported in the Appendix C.

2.4.1 Operative Modes

In order to assess the power consumption of every system for each operative mode of the satellite, it is important to clarify which systems are switched on and which are switched off, as shown in the table below, which only lists the systems that require power to operate.

A detailed description of the satellite's operative modes is given in Table B - 2 and Figure B - 1 in Appendix B.

	PAYLOAD	ADCS	COMSYS	OBC	EPS
DORMANT MODE	OFF	OFF	OFF	OFF	OFF
DETUMBLING MODE	OFF	ON	OFF	ON	ON
COMMISSIONING MODE	ON	ON	ON	ON	ON
BASIC MODE	ON	ON	ON	ON	ON
MISSION MODE	ON	ON	ON	ON	ON
TRANSMISSION MODE	ON	ON	ON	ON	ON

Table 2.3: *On/Off systems per operative mode*

2.4.2 Power Consumption

Once the operative modes of the satellite have been considered, the power consumption of the payload and each subsystem for every operative mode have been collected in the following tables. The power budget calculation has been performed by adopting 10% margins for COTS requiring minor modifications and 20% margins for new designed/developed components, in accordance with the margin philosophy document [7]. Therefore, the power with margin should be considered in the EPS sizing calculations. Furthermore, the Safe, Reconfiguration and Survival modes have not been taken into account both in the power consumption and sizing considerations, because they are not nominal operative

modes, they require less power than other modes and so they are not relevant for the EPS design purposes.

SUBSYSTEM	POWER [W]	MARGIN	POWER WITH MARGIN [W]
PAYLOAD	0	20%	0
ADCS	0.3	20%	0.36
COMSYS	0	20%	0
OBC	1.2	20%	1.44
EPS	0.3	10%	0.33
TOTAL	**1.8**		**2.13**

Table 2.4: *Power consumption in Detumbling Mode*

SUBSYSTEM	POWER [W]	MARGIN	POWER WITH MARGIN [W]
PAYLOAD	5	20%	6
ADCS	1.09	20%	1.31
COMSYS	4.29	20%	5.15
OBC	1.2	20%	1.44
EPS	0.3	10%	0.33
TOTAL	**11.88**		**14.23**

Table 2.5: *Power consumption in Commissioning Mode*

SUBSYSTEM	POWER [W]	MARGIN	POWER WITH MARGIN [W]
PAYLOAD	5	20%	6
ADCS	0.54	20%	0.65
COMSYS	3.71	20%	4.45
OBC	1.2	20%	1.44
EPS	0.3	10%	0.33
TOTAL	**10.75**		**12.87**

Table 2.6: *Power consumption in Basic Mode*

SUBSYSTEM	POWER [W]	MARGIN	POWER WITH MARGIN [W]
PAYLOAD	5	20%	6
ADCS	1.26	20%	1.51
COMSYS	3.71	20%	4.45
OBC	1.2	20%	1.44
EPS	0.3	10%	0.33
TOTAL	**11.47**		**13.73**

Table 2.7: *Power consumption in Mission Mode*

SUBSYSTEM	POWER [W]	MARGIN	POWER WITH MARGIN [W]
PAYLOAD	1	20%	1.2
ADCS	1.09	20%	1.31
COMSYS	4.29	20%	5.15
OBC	1.2	20%	1.44
EPS	0.3	10%	0.33
TOTAL	**7.88**		**9.43**

Table 2.8: *Power consumption in Transmission Mode*

The tables above show the Commissioning Mode as the most demanding operative mode, because both the S-band and the UHF-band of the ComSys operate at their maximum power and all subsystems must be switched on at their nominal power in order to verify proper operation. In the Transmission Mode, the ComSys also operates at maximum power, but the payload consumption is low beacuse it is in idle status. The second most demanding operative mode is the Mission Mode, in which the ADCS requires maximum power to achieve the mission objectives.

2.5 Sizing

The most demanding operative mode and the average consumption have been defined in the previous section in order to conduct the EPS sizing. The worst case takes into account the estimated End Of Life (EOL) power production capability and the selection of an orbit with the maximum eclipse period, chosen from the orbits considered in the two ConOps definition in Section 2.1.

2.5.1 Orbital Parameters

The worst orbital condition of 400 km altitude has been selected because of the higher eclipse period. The calculations of the eclipse and sunlight periods in an orbit have been optained by the analytical expressions. Firstly, the *orbit period* T_{orbit} is affected by the orbit altitude h and it has been calculated with the formula:

$$T_{orbit} = 2\pi \sqrt{\frac{(R_{\oplus}+h)^3}{G \cdot M_{\oplus}}} \quad (1)$$

where $R_{\oplus} = 6371\ km$ is the Earth radius

$G = 6.674 \cdot 10^{-11}\ \frac{Nm^2}{kg^2}$ is the gravitational constant

$M_{\oplus} = 5.972 \cdot 10^{24}\ kg$ is the Earth mass

The *Earth angular radius* ρ is also influenced by the orbit altitude according to the following formulation:

$$\rho = \sin^{-1}\left(\frac{R_\oplus}{R_\oplus + h}\right) \tag{2}$$

The S*un angle* β is defined as the angle between the orbital plane of the satellite and the sun vector. This angle varies between $-90°$ and $+90°$ and depends on four different orbit angles: the *ecliptic true solar longitude* Γ, the *longitude of the ascending node* Ω, the *orbit inclination* i and the *obliquity of the ecliptic* ε.

$$\beta = \sin^{-1}[\cos\Gamma \sin\Omega \sin i - \sin\Gamma \cos\varepsilon \cos\Omega \sin i + \sin\Gamma \sin\varepsilon \cos i] \tag{3}$$

In order to simulate the worst case in terms of maximum time spent in eclipse, a Sun angle of 0° has been chosen.

From the values of *Earth angular radius* ρ and S*un angle* β obtained by equations 2 and 3, the *rotation angle* Φ corresponding to the eclipse duration has been calculated as:

$$\Phi = 2\cos^{-1}\left(\frac{\cos}{\cos\beta}\right) \tag{4}$$

Finally, the *eclipse period* $T_{eclipse}$ and the *sunlight period* $T_{sunlight}$ have been determined according to the following equations:

$$T_{eclipse} = T_{orbit}\frac{\Phi}{360°} \tag{5}$$

$$T_{sunlight} = T_{orbit} - T_{eclipse} \tag{6}$$

The orbital parameters implemented for the sizing analysis are shown in the table below.

PARAMETER	***VALUE***
ORBIT ALTITUDE	$400\ km$
ORBIT INCLINATION	51.6°
THETA ANGLE	$23.5°$
BETA ANGLE	$0°$
ECLIPSE PERIOD	$36.06\ min$
SUNLIGHT PERIOD	$56.39\ min$

Table 2.9: *SILVA mission orbital parameters*

2.5.2 Solar Array Sizing

The solar array sizing must satisfy the power required by both the satellite loads during sunlight periods and the battery recharging energy, in order to guarantee continuous power during eclipse periods and while detumbling. The mission duration of 5 years and the average solar flux of $1367\ W/m^2$ have been considered as fixed dimensioning parameters.

Triple-junction solar cells (InGaP/GaAs/Ge) have been chosen for their high efficiencies and low degradation. The performance of the solar cells considered are as follows:

PERFORMANCE	***VALUE***
IDEAL EFFICIENCY	$28\ \%$
PATH TRANSMISSION EFFICIENCY IN ECLIPSE	0.6
PATH TRANSMISSION EFFICIENCY IN SUNLIGHT	0.8
INHERENT DEGRADATION FACTOR	0.77
DEGRADATION/YEAR	$0.5\ \%$
SPECIFIC POWER DENSITY	$38\ W/kg$

Table 2.10: *Solar cells performance*

The path transmission efficiencies refer to a MPPT regulation type [8].

Once the performance of the solar array has been identified, the sizing parameters have been calculated. The total power that solar array must generate in sunlight, known as the *required solar array power* P_{sa} has been estimated with the analytical formulation:

$$P_{sa} = \frac{\left(\frac{P_{eclipse}T_{eclipse}}{X_{eclipse}} + \frac{P_{sunlight}T_{sunlight}}{X_{sunlight}}\right)}{T_{sunlight}} \tag{7}$$

where $P_{eclipse} = P_{sunlight}$ is the satellite power need during eclipse and sunlight

$X_{eclipse}$ is the path transmission efficiency in eclipse

$X_{sunlight}$ is the path transmission efficiency in sunlight

The *Beginning Of Life* (BOL) *power production capability* P_{BOL} per unit area of the solar array is given by the next espression:

$$P_{BOL} = P_o I_d \cos\theta \tag{8}$$

where the *power output* P_o is the ideal solar cell power output performance per unit area and is equal to the ideal solar cell efficiency times the average solar flux. I_d is

the *inherent degradation factor* defined in Table 2.10, while the angle θ is the *Sun incidence angle* between the normal vector of the array surface and the Sun vector.

The *lifetime degradation* L_d is an estimation of the decline in power production during the satellite's life.

$$L_d = (1 - degradation/year)^{satellite\ life} \tag{9}$$

The *End Of Life* (EOL) *power production capability* P_{EOL} per unit area of the solar array has been calculated with the next formula:

$$P_{EOL} = P_{BOL} \cdot L_d \tag{10}$$

Finally, the *required solar array area* A_{sa} and the *solar array mass* M_{sa} have been estimated as:

$$A_{sa} = \frac{P_{sa}}{P_{EOL}} \tag{11}$$

$$M_{sa} = \frac{P_{sa}}{specific\ power\ density} \tag{12}$$

The solar array sizing parameters obtained are listed in the table below.

PARAMETER	***VALUE***
REQUIRED SOLAR ARRAY POWER	$32.94\ W$
BOL POWER	$270.28\ W/m^2$
EOL POWER	$263.59\ W/m^2$
REQUIRED SOLAR ARRAY AREA	$0.12\ m^2$
SOLAR ARRAY MASS	$0.87\ kg$

Table 2.11: *Solar array sizing*

2.5.3 Battery Sizing

The battery sizing must ensure the power supply required by the satellite loads during eclipse periods. The Depth of Discarghe (DOD), the number of batteries N and the transmission efficiency n have been considered as fixed sizing parameters.

Lithium polymer batteries have been chosen for their high specific energy density and the sizing parameters have been calculated. The *battery capacity* C and the *number of discharge cycles* N_d it endures during the satellite's lifetime have been estimated according to the following expressions:

$$C = \frac{P_{eclipse} T_{eclipse}}{DOD \cdot N \cdot n} \tag{13}$$

$$N_d = \frac{N_{c/d}}{2} \tag{14}$$

where $N_{c/d} = \frac{satellite\ life}{T_{orbit}}$ is the total number of charge/discharge cycles during the satellite lifetime.

The battery performance obtained by the previous calculations are collected in the table below.

PERFORMANCE	***VALUE***
DOD	$40\ \%$
NUMBER OF BATTERIES	2
TRASMISSION EFFICIENCY	0.98
SPECIFIC ENERGY DENSITY	$125\ Wh/kg$
BATTERY CAPACITY	$10.9\ Wh$
NUMBER OF DISCHARGE CYCLES	14224

Table 2.12: *Battery performance and sizing*

2.6 Requirements Definition

Requirements definition is an iterative process that allows a system to be accurately and uniquely defined. This section focuses on the EPS requirements generated by the functional analysis and sizing performed in the previous sections, specifying the expected verification model to be adopted.

The EPS requirements listed below mainly concern functional requirements (Table 2.13), interface requirements (Table 2.14), physical requirements (Table 2.15) and product assurance requirements (Table 2.16).

FUNCTIONAL REQUIREMENTS

ID	**Requirement**	**Verification Model**
FUN-100	The EPS shall supply electrical power to the subsystems	EFM
FUN-110	The EPS shall generate power	EFM
FUN-120	The EPS shall store power	EFM
FUN-125	The EPS shall manage data	EFM
FUN-135	The battery pack shall guarantee 10.90 Wh during eclipse	EFM
FUN-140	The batter pack shall have a maximum DoD of 40%	EFM

FUN-141	The battery pack shall perform at least 28447 charge/discharge cycles	VMU
FUN-145	The solar panels shall provide at least 16.71 Wh to the battery pack during daylight	EFM
FUN-150	The EPS shall distribute electrical power to the subsystems	EFM
FUN-153	The EPS shall provide the subystems a mimimum power of: - 2.13 W in detumbling mode - 14.23 W in commissioning mode - 12.87 W in basic mode - 13.73 W in mission mode - 9.43 W in transmission mode	EFM
FUN-155	The EPS shall mantain four power buses: - one at the battery output voltage of 8.2 V - one at 12 V - one at 5 V - one at 3.3 V	EFM
FUN-157	The 8.2 V power bus shall have one line distributing current at (TBD) A ± (TBD) A to (TBD) load	EFM
FUN-158	The 12 V power bus shall have one line distributing current at 350 mA in transmit and 30 mA in receive to the ComSys	EFM
FUN-159	The 5 V power bus shall have three lines: - one distributing current at 20 mA ± (TBD) A to the ADCS - one distributing current at (TBD) A ± (TBD) A to the OBC - one distributing current at 1.5 A ± 0.3 A to the Payload	EFM
FUN-160	The 3.3 V power bus shall have four lines: - one distributing current at 20 mA ± (TBD) A to the ADCS - one distributing current at 2.7 A ± 0.2 A to the ComSys - one distributing current at (TBD) A ± (TBD) A to the OBC - one distributing current at 1 A ± 0.2 A to the Payload	EFM
FUN-163	The protection diode shall avoid current reversion	EFM

FUN-166	At least one deployment switch shall connect/disconnect the PCU from the battery pack	FM
FUN-168	At least one deployment switch shall connect/disconnect the electrical loads from the battery pack	EFM
FUN-169	A RBF pin shall cut off all power to the CubeSat when inserted into the deployer	EFM
FUN-170	The EPS shall regulate and control electrical power	EFM
FUN-173	Two BCRs shall regulate the electrical power directed from the solar arrays to the battery pack	FM
FUN-174	One SEPIC converter for each BCR shall guarantee: - an output voltage less than the charge voltage limit during battery charge - an output voltage higher than the discharge voltage limit during battery discharge	FM
FUN-175	One MPPT for each BCR shall maximize the output power	FM
FUN-180	The 8.2 V power bus converter shall convert the voltage from variable voltage to 8.2 V	FM
FUN-181	The 12 V power bus converter shall convert the voltage from variable voltage to 12 V	EFM
FUN-182	The 5 V power bus converter shall convert the voltage from variable voltage to 5 V	EFM
FUN-183	The 3.3 power bus converter shall convert the voltage from variable voltage to 3.3 V	EFM
FUN-186	The EPS shall mitigate overcurrent phenomena	EFM
FUN-188	The EPS shall protect the loads from shortcircuits	EFM
FUN-192	The EPS ADC shall convert analog data from the solar arrays, the battery pack and the LCLs into digital data	EFM/FM
FUN-195	The EPS MCU shall collect digital data from the EPS ADC	EFM
FUN-196	The EPS MCU shall exchange data with the CAN-bus 1	FM
FUN-197	The EPS MCU shall send commands to every LCLs	FM

FUN-199	The EPS maximum power consumption shall be less than or equal to: - 0.3 W in detumbling mode - 0.3 W in commissioning mode - 0.3 W in basic mode - 0.3 W in mission mode - 0.3 W in transmission mode	EFM

Table 2.13: *EPS functional requirements*

INTERFACE REQUIREMENTS

ID	Requirement	Verification Model
INT-050	The 104-pins connectors shall transfer electrical power from EPS board to the subsystems boards	FM
INT-052	The electrical wires shall transfer electrical power from the solar panels to the EPS board	EFM
INT-055	The electrical wires shall transfer electrical power from the EPS board to the battery pack	EFM
INT-160	I2C-protocol shall be used to transfer commands from the EPS MCU to every LCLs	FM

Table 2.14: *EPS interface requirements*

PHYSICAL REQUIREMENTS

ID	Requirement	Verification Model
PHY-052	The total solar array area shall be at least 0.125 m^2 ± 5%	FM
PHY-075	The EPS board battery pack shall totally weight less than 335 g ± 5%	FM
PHY-077	The EPS board shall weight less than 86 g ± 5%	FM
PHY-084	The total solar array mass shall be less than 870 g ± 5%	FM

Table 2.15: *EPS physical requirements*

PRODUCT ASSURANCE REQUIREMENTS

ID	Requirement	Verification Model
PRA-020	The LCLs shall protect the loads from undervoltage	FM
PRA-021	The LCLs shall protect the loads from overcurrent	FM
PRA-022	The LCLs shall protect the loads from shortcircuit	FM

Table 2.16: *EPS product assurance requirements*

3 Development and Manufacturing

The design of the EPS and the requirements elicitation lead to the selection of a final configuration that meets both the system sizing and the derived requirements. This chapter focuses on the hardware development of the EPS, providing a Flight Model (FM) to be adopted in further developments and an Electrical and Functional Model (EFM), realised with preliminary components and used for the requirements verification, illustrated in the next chapter. Furthermore, the software development played an important part in the requirements verification and test execution and focused mainly on codes for commanding the power bench, data acquisition, data conversion and processing of the converted data.

3.1 Flight Model

Considering the preliminary configuration study, the solar array and battery sizing, and the requirements defined, a configuration consistent with the studies made in the previous chapter has been chosen. The selected configuration guarantees sufficient power supply to satisfy the satellite's power need for its whole life in orbit, and represents the EPS flight model, consisting of COTS components listed below. However, their characteristics are fully presented in Appendix A.

- Low-Cost Triple-Junction solar cells (CTJ-LC) from CESI [9] company have been selected.

Figure 3.1: *CTJ-LC solar cell [9]*

Cell Area	$30.15\ cm^2$
BOL Efficiency	38 %
$\boldsymbol{V_{oc}}$	$2.62\ V$
$\boldsymbol{V_{mp}}$	$2.32\ V$
$\boldsymbol{I_{sc}}$	$520\ mA$
$\boldsymbol{I_{mp}}$	$496\ mA$

Table 3.1: *CTJ-LC features*

- Optimus-30 battery from AAC Clyde Space [10] company has been selected.

Figure 3.2: *Optimus-30 battery [10]*

Cell Type	LiPo
Mass	$268\ g$
Typical Capacity	$30\ Wh$
Max Discharge Rate	$1.95\ A$
Charge Voltage Limit	$8.4\ V$
Discharge Voltage Limit	$6.2\ V$

Table 3.2: *Optimus-30 features*

- Starbuck-Nano board from AAC Clyde Space [10] company has been selected.

Figure 3.3: *Starbuck-Nano board [10]*

Input Voltages	$3\ to\ 30\ V$
Output Voltages	$3.3\ /\ 5\ /\ 12\ V$
Max Efficiency	$92\ \%$
Number of LCLs	10
Mass	$86\ g$

Table 3.3: *Starbuck-Nano features*

3.2 Electrical and Functional Model

The electrical and functional model of the EPS has been manufactured in the Systems and Technologies for Aerospace Research laboratory (STARlab) at the Department of Mechanical and Aerospace Engineering (DIMEAS) of the Politecnico di Torino. Firstly, the EPS components available in the STARlab have been examined and those most suitable to the case study have been chosen. The features of the hardware selected are described in more detail as follows.

3.2.1 Solar panel

Three solar panels for a 1U CubeSat, consisting of two solar cells each, have been selected, because a minimum of six solar cells was necessary in order to simulate at least one face of the 3U CubeSat. The selected triple-junction (InGaP/GaAs/Ge) solar cells come from CESI company and are shown in Figure 3.4. Moreover, their characteristics are listed in Table 3.4.

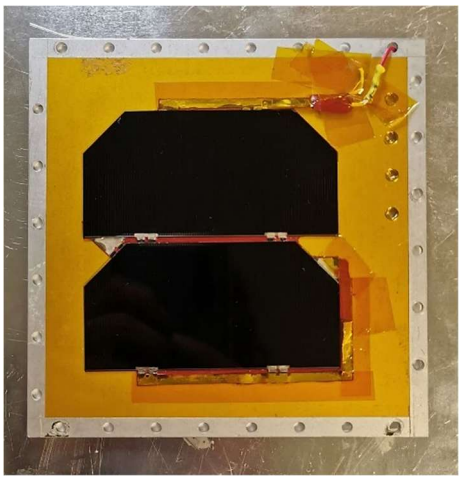

Figure 3.4: *A solar panel with two solar cells*

Cell dimension	$8\ cm\ x\ 4\ cm$
Solar panel dimension	$12.6\ cm\ x\ 12.6\ cm$
BOL Efficiency	$27.8\ \%$
$\boldsymbol{V_{oc}}$	$2.60\ V$
$\boldsymbol{V_{mp}}$	$2.34\ V$
$\boldsymbol{I_{sc}}$	$454.67\ mA$
$\boldsymbol{I_{mp}}$	$427.36\ mA$
$\boldsymbol{P_{max}}$	$998.1\ mW$
Fill factor	0.845

Table 3.4: *Solar cells characteristics*

The three solar panels have taken part of an assembly process, considered as part of the AIV plan, that will be fully described more in detail in the next chapter. The solar panels assembly consists of three macro steps:

- A structural unification of the three panels, starting with the initial measurement of the panels and the subsequent overlapping of the structure empty of solar cells, obtaining a distance of 30 cm between the first cell and the last one;
- A structural support development, in order to maintain the solar panel in a stable equilibrium on the horizontal plane;
- An electrical connection in series of the solar cells.

That process results in a unique solar panel made of 6 solar cells, as shown in Figure 3.5. In addition, the step-by-step procedure for that assembly is described in Table D - 1 in Appendix D.

Figure 3.5: *Solar panel with six solar cells*

3.2.2 Battery pack

A battery pack consisting of 6 cells has been considered, in which 3 cells are connected in series and then the 2 pairs of three cells are connected in parallel (3S2P). The battery pack shown in Figure 3.6 comes from Ansmann company and its characteristics are collected in Table 3.5.

Figure 3.6: *Battery pack*

Cell type	Li-ion
Number of cells	6 (3S2P)
Nominal Voltage	$11.1\ V$
Max Charge Voltage	$12.6\ V$
Nominal Capacity	$5.2\ Ah$
Minimum Capacity	$5\ Ah$
Energy	$57.7\ Wh$

Table 3.5: *Battery pack characteristics*

3.2.3 EPS board

The EPS board has been produced by AT Automation Srl company and the main items are 2 solar panel access ports, 2 battery pack access ports, 1 load port, and a 104-pin connector. The board has no MPPT and this is the major difference compared to the flight model. A front and rear view of the board are shown in Figure 3.7 and Figure 3.8, respectively. In addition, some features of the board are collected in the Table 3.6.

Figure 3.7: *Front view of the EPS board*

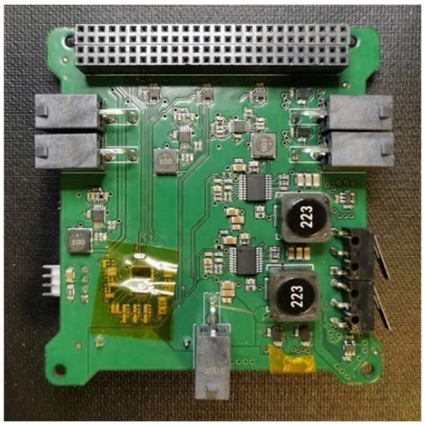

Figure 3.8: *Rear view of the EPS board*

Maximum Solar Panel Input Voltage	$20\ V$
Output Voltages	3.3 / 5 / 9 / 12 V
Number of switches	2
Number of RBF pin	1

Table 3.6: *EPS board characteristics*

3.2.4 Voltage/Current measure board

The voltage/current measure board has been manufactured in the STARlab and consists of two differential amplifiers, made with two operational amplifiers (op amp) in simple differential configuration. One op amp measures the voltage from the solar panel, amplifying it with a gain $G < 1$. The other op amp measures the solar panel current, by passing it through a $0.1\ \Omega$ shunt resistor, out of which the voltage will be amplified with high gain. The solar panel voltage and the voltage generated in the shunt are then raised to values that can be measured by the Arduino's ADC. A picture of the voltage/current measure board is shown in the figure below.

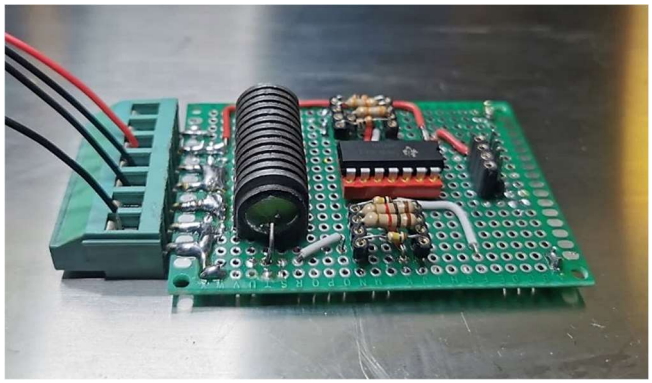

Figure 3.9: *Voltage/current measure board*

3.3 Software Development

The software development used to verify the requirements by performing the tests, described in the next chapter, focused on the development of five main codes:

- An Arduino sketch, designed to run on the Arduino's ADC and which enabled the acquisition of digital data, readed by the ADC on the EPS board;
- An Arduino sketch, to be run on the Arduino's ADC in order to acquire the digital data from the voltage/current measure board. This code acquires the raw data and processes them into real data, while printing both the raw and transformed data on the PC screen. The output values also include the measured resistance value, calculated using the first Ohm's law.
- A C code that allows the communication with the power bench, sending as input the voltage and current values it has to deliver from its first 2 output channels. Indeed, the power bench simulates the sun, reproducing the orbital conditions of sunlight and eclipse periods to which the satellite is subjected.
- A Python code, scripted to allow the conversion of raw data into real data. The data conversion is performed by means of coefficients obtained from the data calibration and the datasheet of the EPS board.
- A Matlab script, which allows the data processing of the real data obtained, importing them from text files and plotting the test results.

4 Analysis and Test Verification

The electrical and functional model presented in the previous chapter has been the subject of a test campaign, conducted in order to verify most of the EPS requirements. Firstly, verification tests on the individual components have been conducted, to perform the solar panel and battery pack characterisation, the EPS board acceptance and to verify their functionality. Afterwards, integration tests have been carried out in order to verify the functioning of at least two integrated components. This chapter aims to explain the AIV plan defined for the whole EPS test campaign, continuing with the description of each test conducted and the obtained results.

4.1 AIV plan

The AIV plan is an assembly, integration and verification programme, whose planning begins when the system design is finalised. The AIV plan's purposes are the test objectives statement, the test verification description, the definition of the test sequences, the test execution management and the step-by-step procedures documentation, specifying the test facilities and the implemented tools.

The requirements verification requires a bottom-up approach, from the component-level up to the system-level, taking into account both the verification models adopted and the four applicable verification methods:

- Analysis (A), which entails performing a theoretical or empirical evaluation using accepted analytical techniques. The selected techniques may typically include systematics, statistics, qualitative design analysis, modelling and computer simulation.
- Inspection (I), that determines conformance to requirements for construction features, documents and drawing conformance, workmanship and physical condition without the use of laboratory equipment, procedures or services.
- Testing (T), that allows requirements to be verified by measuring product performance and functions in various simulated environments.
- Review of design (R), that applies validation of previous records or evidence of validated design documents, when approved design reports, technical descriptions and engineering drawings unequivocally demonstrate that the requirement is met.

The flow of activities planned for the EPS test campaign is now described, starting with characterisation and acceptance tests performed on the individual components, continuing with the integration of the components, up to the final EPS integration test. The first planned step is the integration between the EPS board and the Arduino board,

resulting in an acceptance test during which the functionalities of the two boards shall be confirmed. Afterwards, the battery pack is tested through a charge test. Next, the EPS board, the Arduino board and the battery pack are integrated with a resistive load, which allows both a battery discharge test and a sun simulation test to be performed. Then, the integration of the solar panel and a voltage/current measure board results in the illumination test to demonstrate the solar panel performance, and finally, the integration to the previous components shall be performed, resulting in the EPS integration test. The activity flow described is illustrated in Figure 4.1.

The test campaign has been performed in two different facilities: the main one has been the Clean Room at the STARlab, which is an insulated ISO class 7 room, with a volume of 60 m^3 and a 20 m^2 floor area, equipped with appropriate desks, chairs, shelves and equipment and can accomodate up to three operators. The Clean Room has been used for the assembly and integration of the test items and for the execution of tests that did not require the Sun, and the environmental conditions during the verification activities have been registered in terms of:

- Temperature: 25 °C
- Atmospheric pressure: 985 hPa
- Air humidity: 75 %

On the other hand, the second facility has been an outdoor area of the Politecnico di Torino, which had good accessibility to sunlight in order to perform the illumination test and the EPS integration test, which require the Sun as an integral part of the test. The environmental conditions of the second facility have been:

- Temperature: 15 °C
- Atmospheric pressure: 974 hPa
- Air humidity: 30 %

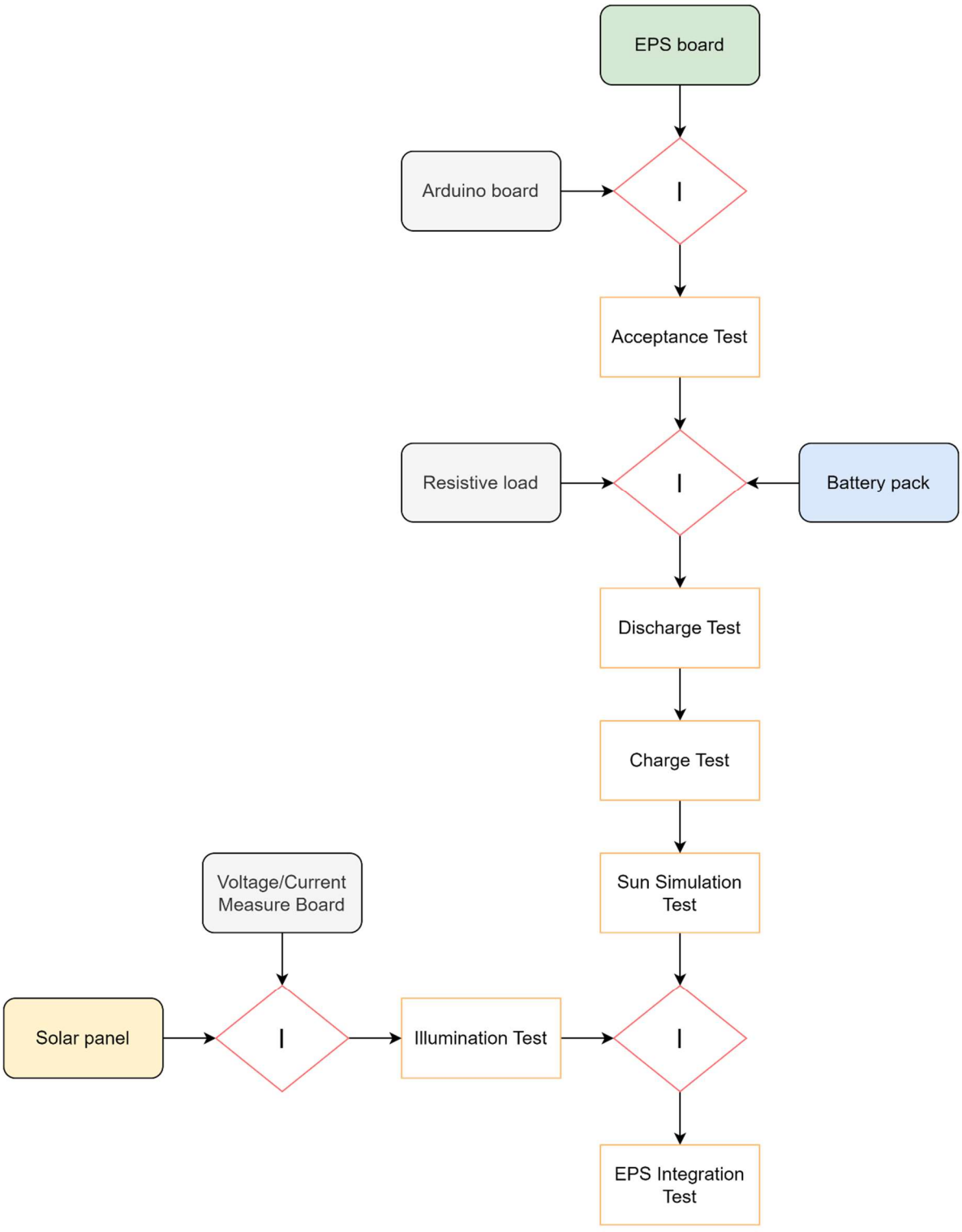

Figure 4.1: *AIV plan activity flow of the EPS test campaign*

4.2 Battery Discharge Test

4.2.1 Test objective

The objectives of the battery discharge test aims to verify:

- EPS board telemetry acquisition;
- Battery pack discharging.

A breakdown of the requirements to be verified for these objectives is presented in the table below.

What to verify	How to verify	Requirements ID to be verified
EPS board data acquisition	Data evaluation	FUN-125, FUN-192, FUN-195
EPS board power regulation	Data evaluation, direct measurement with GSE	FUN-100, FUN-170, FUN-182, FUN-183
EPS board power distribution	Data evaluation, direct measurement with GSE	FUN-100, FUN-150, FUN-155, INT-055
Battery discharging	Data evaluation	FUN-100, FUN-135, FUN-140, FUN-145, FUN-153

Table 4.1: *EPS requirements to be verified in the battery discharge test*

4.2.2 Test setup

The equipment employed for the setup of the battery discharge test are:

- Battery pack, described in Section 3.2.2;
- EPS board, described in Section 3.2.3;
- Arduino Nano board;
- Breadboard;
- Resistor;
- PC.

In addition, in the AIV process of the battery discharge test, Ground Support Equipment (GSE) has been used and are described in Table 4.2.

EQUIPMENT	Comments
Multimeter	To do direct measurements
Connectors	To connect components
Welder	To fix connectors and wires
Welding wire	To perform welding
Crimper	To crimp connector and wire
Jump wires	To interconnect components
Kapton tape	To protect exposed connections
Scissors	To cut the Kapton tape
NTC thermistor	To measure battery pack temperature
USB-A/Mini-B cable	To connect the PC to the Arduino Nano board
Anti-static mat	To protect components from ESD

Table 4.2: *GSE required in the battery discharge test*

The battery discharge test setup requires the battery pack to be connected to the EPS board through the first battery pack access port. The constant load consists of a resistor equipped with a connector compatible with the load access port of the EPS board. The Arduino Nano board is the interface between the EPS board and the PC, and allows a SPI communication line via jump wires. The PC communicates with the Arduino board through the USB-A/Mini-B cable, connected to the USB0 port of the PC. Via the same cable, the PC supplies 5 V to the Arduino board.

Hereafter, the block scheme show how the test equipment shall be connected and the interface between them.

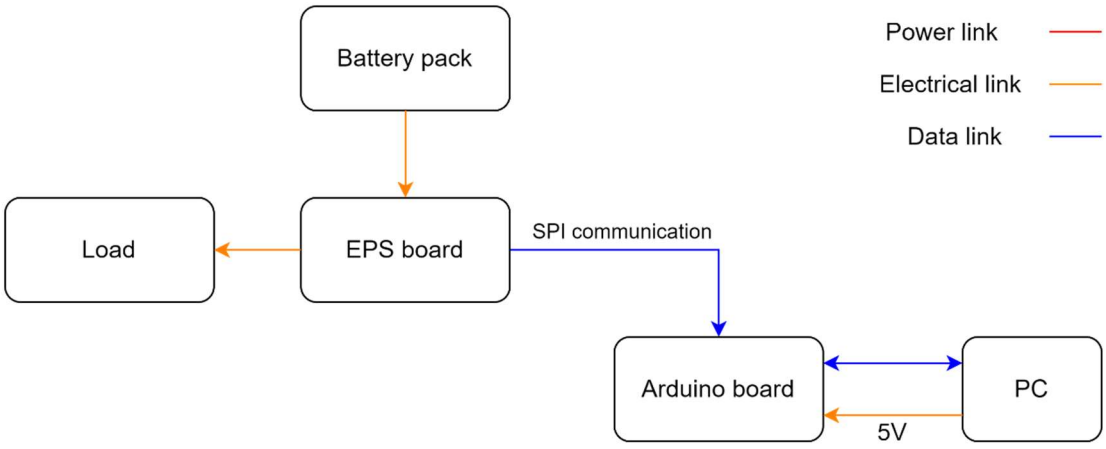

Figure 4.2: *Block scheme of the battery discharge test*

4.2.3 Test execution

Before starting the test, the battery voltage has been measured with a multimeter, resulting in:

$$V_{battery} = 12.71\ V$$

Hence, the battery pack resulted fully charged. Next, some analytical calculations have been performed to select the resistor value to be used in the test and to estimate the test duration, considering diffent values of the maximum current and resistors to be used. The calculations performed are described in Appendix E, while the Table 4.3 shows the results obtained, by assuming the resistors available in the STARlab as a constraint.

Resistor value [Ω]	Max power dissipation [W]	Max current [mA]	C - rate	Time for fully discharge [h]
8.3	1/2	1500	0.3	3.5
10	2	1270	0.24	4.1
15	3	850	0.16	6.3
30	50	420	0.08	12.4
47	23	270	0.05	19.3
67	23	190	0.04	27.4
220	1/4	58	0.01	89.7

Table 4.3: *Calculations for resistor selection*

The 30 Ω resistor has been selected as the resistive load for the battery discharge test execution, because it represents the best solution between high power dissipation and low discharge time.

Afterwards, the Arduino sketch has been compiled and the resulting executable file has been run through the minicom terminal on the PC. The Arduino board started reading zero values from the ADC on the EPS board every second and these values have been displayed on the PC screen. The load, the battery pack and the NTC thermistor have been connected to the EPS board and the values have been read by the PC's terminal.

An anomaly encountered concerned the resistor, which started to overheat soon after the start of the test. To overcome that, a cold aluminium plate has been placed under the resistor and a heat sink compound has been applied between the resistor and the plate.

Finally, Figure 4.3 and Figure 4.4 show photos taken during the battery discharge test execution.

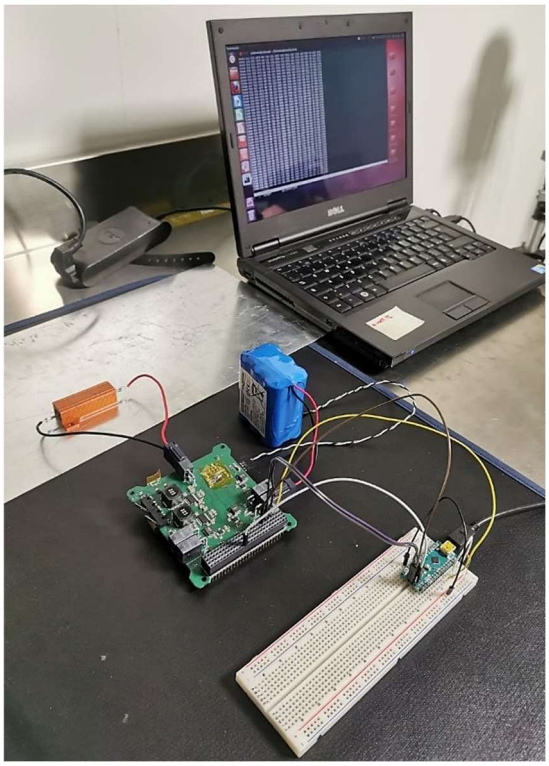

Figure 4.3: *Battery discharge test execution*

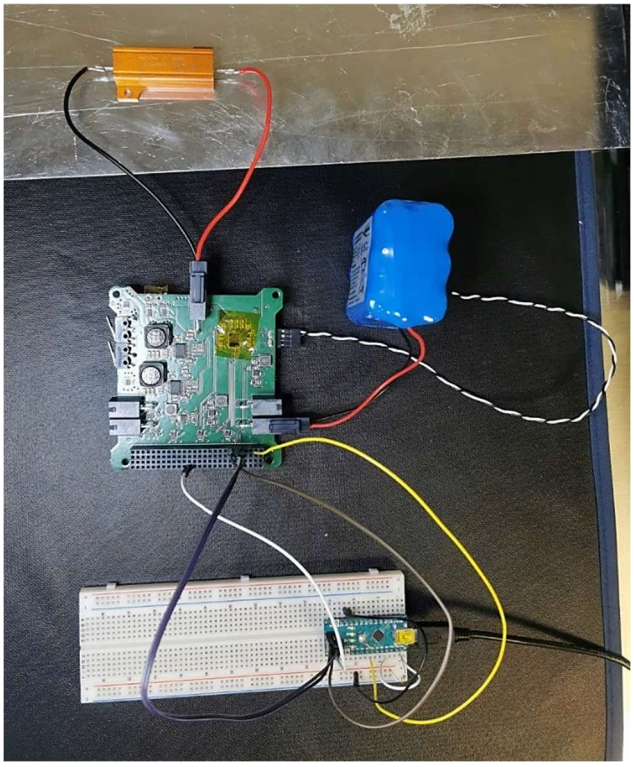

Figure 4.4: *Zoom on interfaces during the battery discharge test execution*

4.2.4 Test result

Once the test had been finished, the raw data obtained had been saved in a text file. Post-processing of the data has been then carried out, in order to get the real data, using a Python code described in more detail in the Section 3.3. The real data obtained have been elaborated by Matlab, which made it possible to produce the result plots, shown below.

Figure 4.5 shows the battery discharge voltage and current during the battery discharge test, which has been performed in about 14 hours total, over 2 days. From the plot, a discontinuity is noticeable after about 8 hours of discharge, which indicates the point at which the test has been stopped and restarted the next day. Moreover, in the final area of the current curve there are many fluctuations, due to the 9 V supply line regulator on the EPS board, not having a high enough input voltage to properly work, as evident in the Figure 4.6. Instead, the final area of the battery discharge voltage curve goes down rapidly due to the Battery Management System (BMS) inside the battery pack, which has been activated to disconnect the battery, preventing any damage.

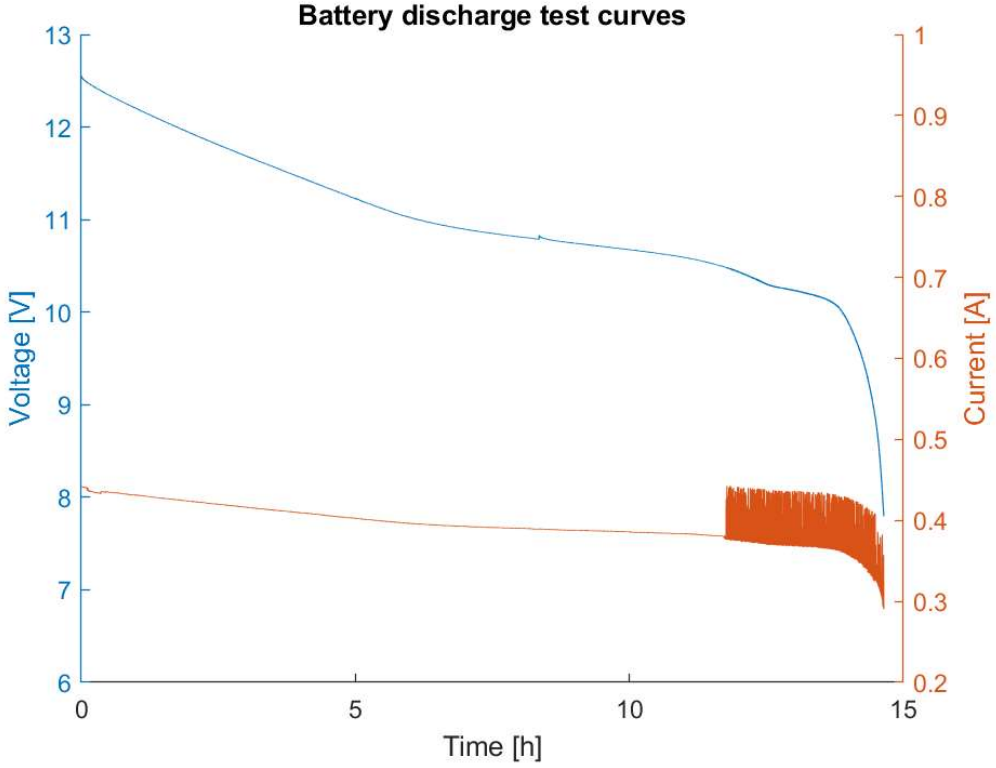

Figure 4.5: *Battery discharge test results*

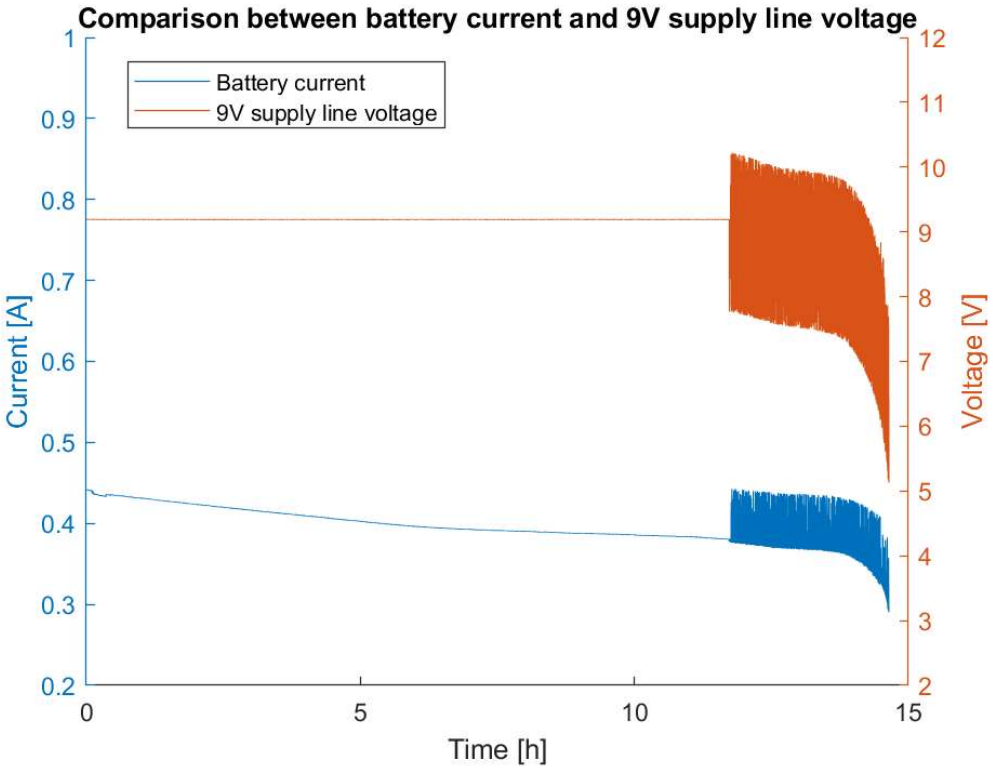

Figure 4.6: *Origin of battery discharging current fluctuations*

The battery temperature has also been monitored during the battery discharge test. In Figure 4.7, a gradual increase in temperature is evident and a discontinuity of 3°C can be seen, due to the interruption of the test and its restart a day later.

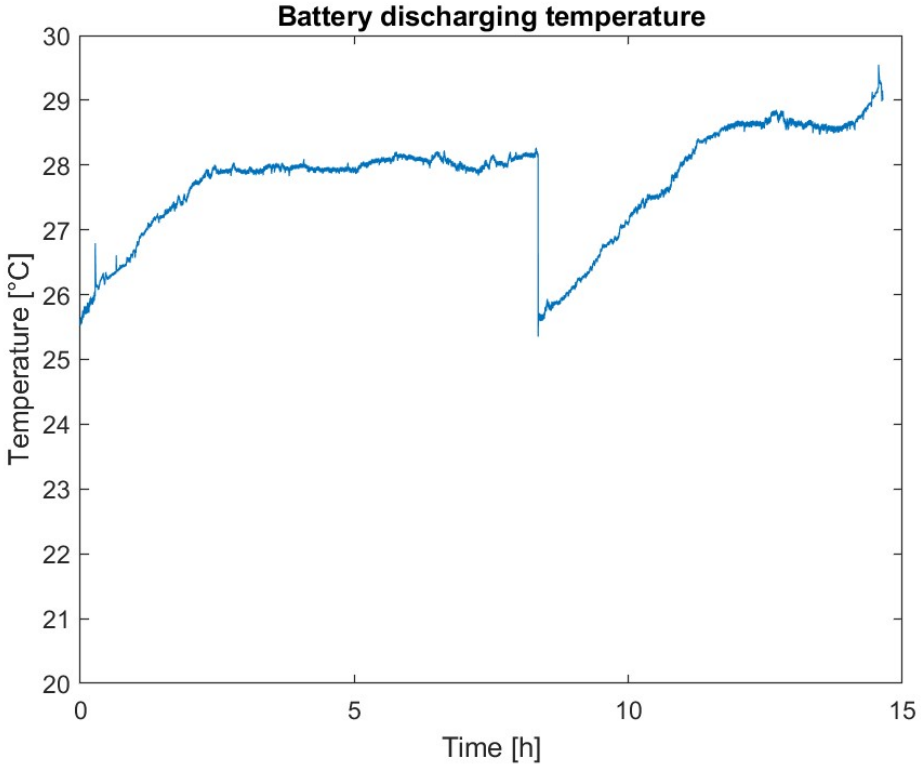

Figure 4.7: *Battery temperature during battery discharge test*

4.3 Battery Charge Test

4.3.1 Test objective

The objectives of the battery charge test aims to verify:

- EPS board telemetry acquisition;
- Battery pack charging.

What to verify	How to verify	Requirements ID to be verified
EPS board data acquisition	Data evaluation	FUN-125, FUN-192, FUN-195
EPS board power regulation	Data evaluation, direct measurement with GSE	FUN-170, FUN-173, FUN-182, FUN-183
EPS board power distribution	Data evaluation, direct measurement with GSE	FUN-155, INT-055
Battery charging	Data evaluation	FUN-120, FUN-145, FUN-173, INT-055

Table 4.4: *EPS requirements to be verified in the battery charge test*

4.3.2 Test setup

The equipment employed for the setup of the battery charge test are:

- Battery pack, described in Section 3.2.2;
- EPS board, described in Section 3.2.3;
- Power bench;
- Arduino Nano board;
- Breadboard;
- PC.

GSE are described in the table below.

EQUIPMENT	Comments
Multimeter	To do direct measurements
Connectors	To connect components
Welder	To fix connectors and wires
Welding wire	To perform welding
Crimper	To crimp connector and wire
Crocodile clips	To connect the power bench
Jump wires	To interconnect components

Kapton tape	To protect exposed connections
Scissors	To cut the Kapton tape
NTC thermistor	To measure battery pack temperature
USB-A/Mini-B cable	To connect the PC to the Arduino Nano board
Anti-static mat	To protect components from ESD

Table 4.5: *GSE required in the battery charge test*

The battery charge test setup requires the power bench to be connected to the EPS board in the first solar panel access port. The crocodile clips guarantee that connection and the voltage value in channel 1 of the power bench is set 20% higher than the nominal voltage of the battery pack, ensuring battery charging. The battery pack shall be connected to the EPS board through the first battery pack access port. The Arduino Nano board is the interface between the EPS board and the PC, and allows a SPI communication line via jump wires. The PC communicates with the Arduino board through the USB-A/Mini-B cable, connected to the USB0 port of the PC. Via the same cable, the PC supplies 5 V to the Arduino board.

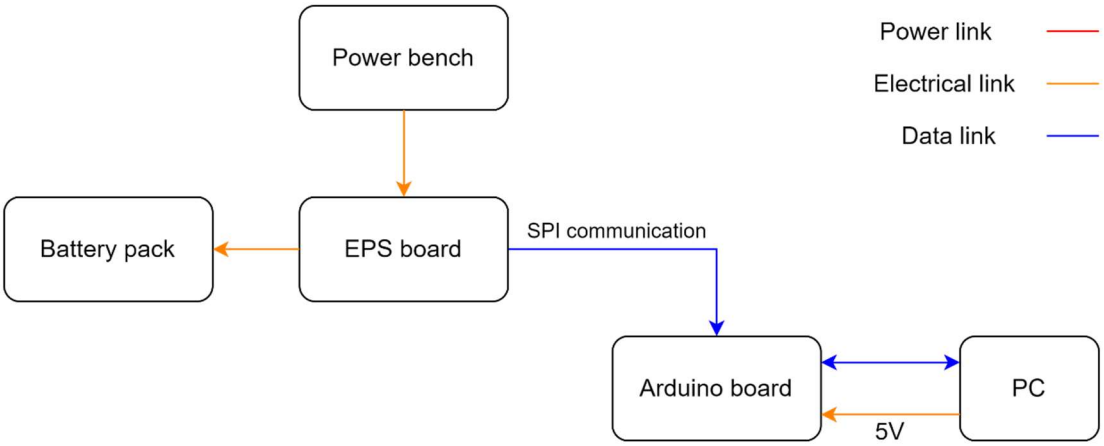

Figure 4.8: *Block scheme of the battery charge test*

4.3.3 Test execution

First of all, the channel 1 of the power bench has been set to the following values:

- Voltage @ 13.32 V
- Current @ 1 A
- Overcurrent protection @ 13.50 V

Then, the Arduino sketch has been compiled and the resulting executable file has been run through the minicom terminal on the PC. The Arduino board started reading values from the ADC on the EPS board every second and these values have

been displayed on the PC's terminal. Finally, the battery pack and the NTC thermistor have been connected to the EPS board.

During the battery charge test, no anomalies have been detected.

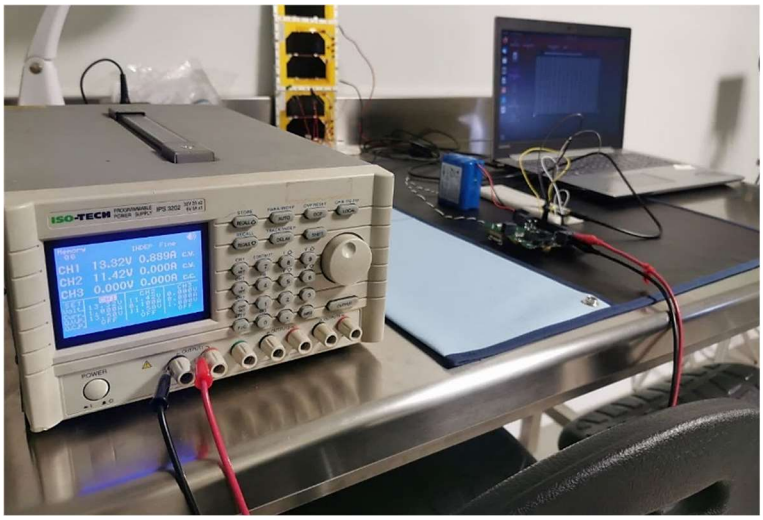

Figure 4.9: *Power bench in the battery charge test execution*

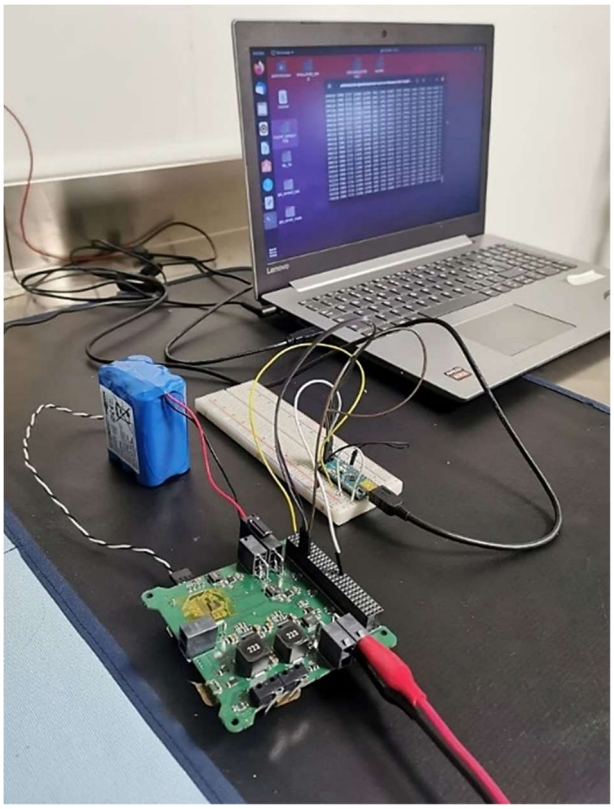

Figure 4.10: *Battery charge test execution*

4.3.4 Test result

The battery charge test has been performed in almost 10 hours, over 3 days, which is why two discontinuities can be seen for both the voltage in Figure 4.11 and temperature in Figure 4.12.

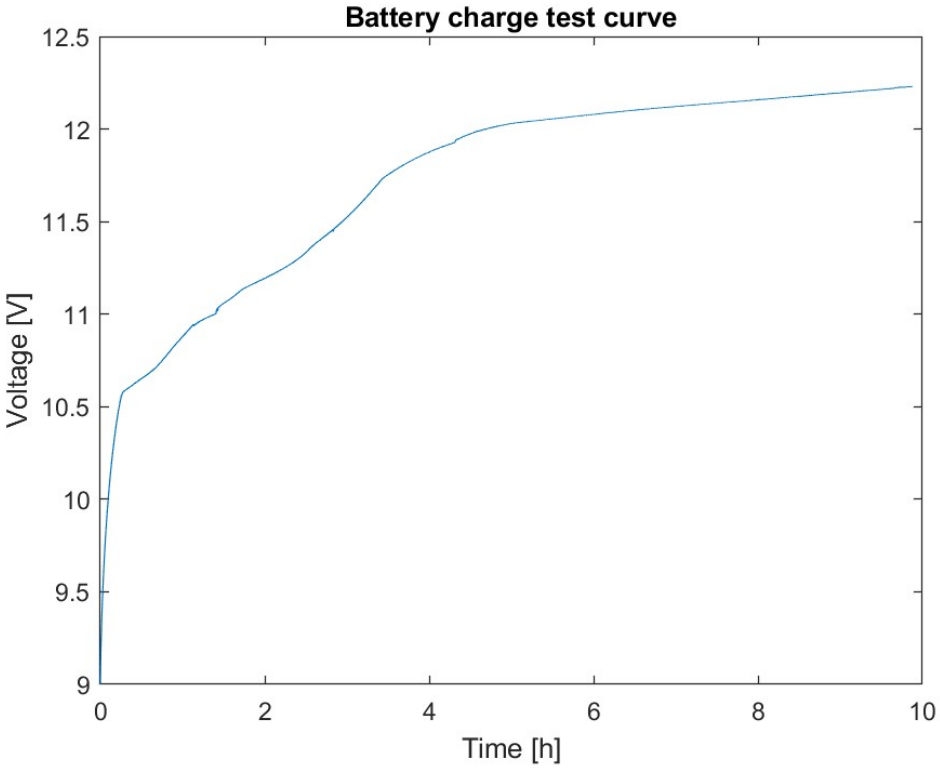

Figure 4.11: *Battery charge test results*

The battery charging voltage is consistent with the ideal curve, but the test performed only provides the constant current (CC) charging phase. Indeed, the contant voltage (CV) charging phase, which would have caused the curve to stabilise at a voltage value around $12.6\ V$, is missing.

The battery temperature has been monitored during the battery charge test and a gradual increase is noted as a general trend. In the second charging section, a temperature peak of about $31.2\ °C$ is noted and then a slight decrease, probably due to the NTC sensor being easily influenced by the ambient temperature. The most reliable behaviour is found in the third charging section, where the temperature increases from about $26.5\ °C$ to $29.6\ °C$.

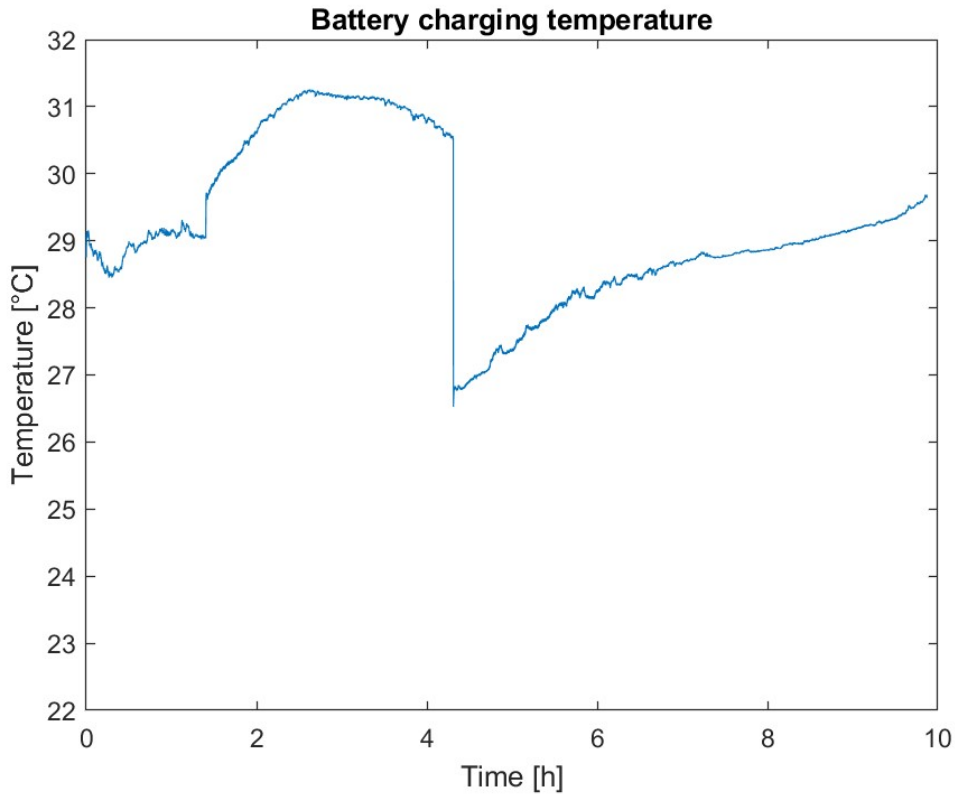

Figure 4.12: *Battery temperature during battery charge test*

4.4 Illumination Test with direct sunlight

4.4.1 Test objective

The objectives of the illumination test with direct sunlight aims to verify:

- Solar panel electrical characteristics;
- Solar panel power providing.

What to verify	How to verify	Requirements ID to be verified
Solar panel power generation	Data evaluation, direct measurement with GSE	FUN-110, FUN-145, FUN-153

Table 4.6: *EPS requirements to be verified in the illumination test with direct sunlight*

4.4.2 Test setup

The equipment employed for the illumination test with direct sunlight setup are:

- 3U solar panel, described in Section 3.2.1;
- Arduino Uno board;
- Breadboard;
- Voltage/current measure board, described in Section 3.2.4;
- Resistors;
- PC.

GSE described in Table 4.7, has been used in the assembly, integration and verification process of the illumination test.

EQUIPMENT	Comments
Metal supports with threaded holes	For solar panel assembly
Threaded screws	For solar panel assembly
Nuts	For solar panel assembly
Screwdrivers	To fix the screws
Red wire	For electrical connection
Black wire	For electrical connection
Multimeter	To do direct measurements
Connectors	To connect components
Welder	To fix connectors and wires
Welding wire	To perform welding
Heat shrinkable tubing	To protect welded wires
Crimper	To crimp connector and wire

Jump wires	To interconnect components
Goniometer	To measure the solar panel inclination
Kapton tape	To protect exposed connections
Scissors	To cut the Kapton tape
USB-A/USB-B cable	To connect the PC to the Arduino Uno board
Anti-static mat	To protect components from ESD

Table 4.7: *GSE required in the illumination test with direct sunlight*

The illumination test with direct sunlight requires solar panel to be exposed to the Sun. The solar panel shall be connected to the breadboard via jump wires. In the breadboard several resistors combinations are connected to the voltage/current measure board through wires. The Arduino Uno board is the interface between the voltage/current measure board and the PC, and allows the analog data acquisition from the voltage/current measure board via jump wires. The PC communicates with the Arduino board through the USB-A/USB-B cable, connected to the USB0 port of the PC. Via the same cable, the PC supplies 5 V to the Arduino board. In turn, the Arduino board supplies 5 V to the voltage/current measure board via jump wires.

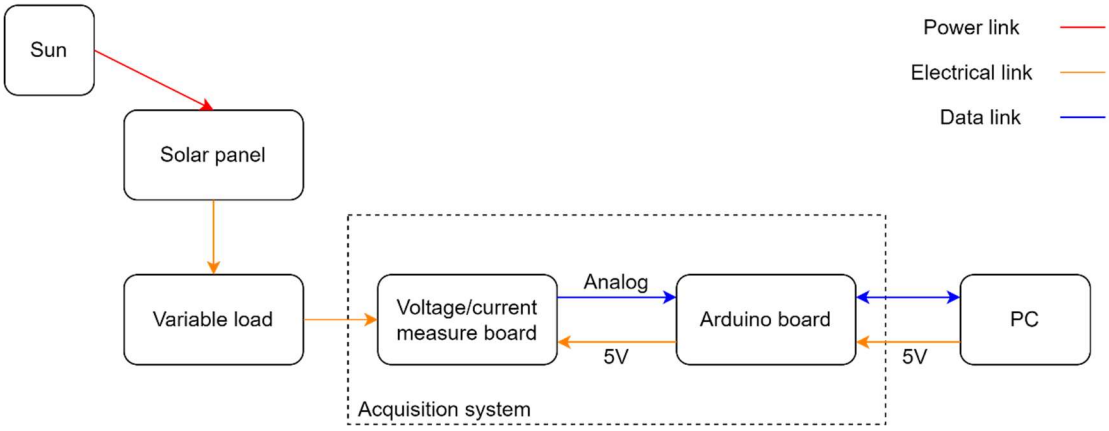

Figure 4.13: *Block scheme of the illumination test with direct sunlight*

4.4.3 Test execution

Before starting the test, some considerations on the variable load implementation have been made. A wide combination of resistor values has been considered to be fixed in the breadboard, assuming that one of the wires of the voltage/current measure board had to be moved during the test execution in order to simulate a variable load. Therefore, 25 resistors have been chosen, obtaing the value combinations listed in the first column of Table 4.8. In each row of the second column, the resistors used have to be intended as in series with the resistor values

of the previous rows (e.g. a 10 Ω resistor in series with two 8.3 Ω resistors in parallel gives a load value of 15.3 Ω, and so on).

LOAD VALUE [Ω]	RESISTORS USED
10.2	A 10 Ω resistor
15.3	In series with two 8.3 Ω resistors in parallel
20.6	In series with two 8.3 Ω resistors in parallel
26.2	In series with two 10 Ω resistors in parallel
31.7	In series with two 10 Ω resistors in parallel
36.7	In series with two 10 Ω resistors in parallel
41.4	In series with two 10 Ω resistors in parallel
49.4	In series with two 15 Ω resistors in parallel
58.3	In series with a 8.3 Ω resistor
68.3	In series with a 10 Ω resistor
115	In series with a 47 Ω resistor
162.3	In series with a 47 Ω resistor
273.8	In series with two 220 Ω resistors in parallel
425	In series with two 301 Ω resistors in parallel
575	In series with two 301 Ω resistors in parallel

Table 4.8: *Variable load implementation for the illumination test execution*

The breadboard with the resistors implemented is shown in the figure below, together with the components interfaces during the illumination test execution.

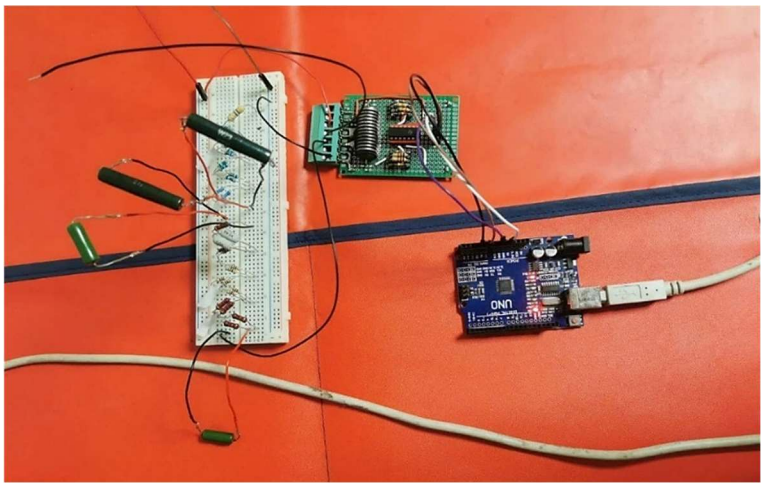

Figure 4.14: *Zoom on interfaces during the illumination test execution*

The solar panel has been tilted by about 75° in order to generate the maximum power. Then, the open-circuit voltage has been measured through a multimeter before the test began. The Arduino script has been run on the PC, starting to acquire data, while the voltage/current measure board wire has been fixed for about 10

seconds at each load value described in Table 4.8, thus ensuring at least 4 data acquisitions on average per load.

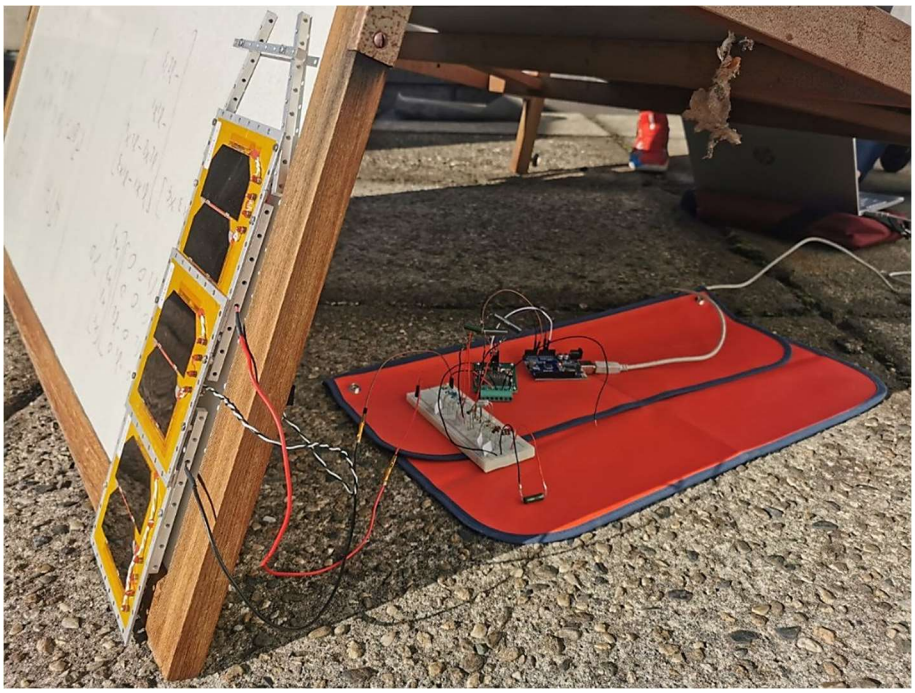

Figure 4.15: *Illumination test execution with direct sunlight*

4.4.4 Test result

The illumination test with direct sunlight allows to obtain the I-V and the P-V curves, that characterise the solar panel. On the P-V curve, the maximum power P_{max} has been identified and plotted on the I-V curve, identifying the MPP and the corresponding current at maximum power I_{mp} and voltage at maximum power V_{mp}. In addition, the point at which the voltage value is maximum and the current value is zero represents the open circuit voltage V_{oc}. The values obtained are shown in the table below.

$\boldsymbol{P_{max}}$	$\mathbf{3.38\ W}$
$\boldsymbol{I_{mp}}$	$282\ mA$
$\boldsymbol{V_{mp}}$	$12.02\ V$
$\boldsymbol{V_{oc}}$	$14.25\ V$

Table 4.9: *Characteristic points from the illumination test with direct sunlight*

As evident from Figure 4.16, the initial slope of the I-V curve is indication of shunt losses, as a decrease in shunt resistance leads to an increase in the slope of the I-V curve. Therefore, the shunt resistor on the voltage/current measure board probably has influenced the slope of the curve. On the other hand, the final slope of the I-V

curve in the proximity of V_{oc} is typical of series losses due to the resistors employed. However, no step-like behaviour is observed, which is typical of shading and electrical mismatch losses between the cells.

Finally, a greater thickening of the intervals between the resistance values is recommended, as it would have ensured a better characterisation of the curves.

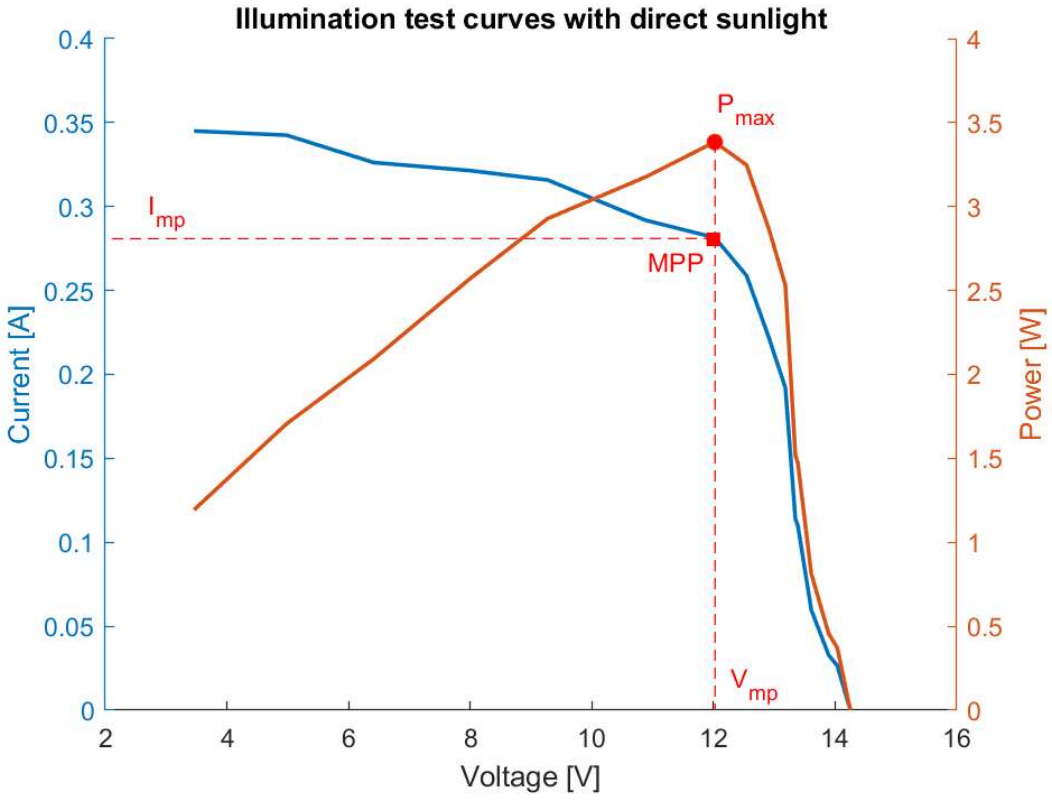

Figure 4.16: *I-V and P-V curves of the illumination test with direct sunlight*

4.5 Illumination Test with incandescent lamp

4.5.1 Test objective

The objectives of the illumination test with incandescent lamp aims to verify:

- Solar panel electrical characteristics;
- Solar panel power providing.

What to verify	How to verify	Requirements ID to be verified
Solar panel power generation	Data evaluation, direct measurement with GSE	FUN-110, FUN-145, FUN-153

Table 4.10: *EPS requirements to be verified in illumination test with lamp*

4.5.2 Test setup

The equipment employed for the setup of the illumination test with incandescent lamp are:

- 3U solar panel, described in Section 3.2.1;
- Arduino Uno board;
- Breadboard;
- Voltage/current measure board, described in Section 3.2.4;
- Resistors;
- Incandescent lamp;
- PC.

Further GSE for the assembly, integration and verification process of the illumination test with incandescent lamp are described in Table 4.11.

EQUIPMENT	Comments
Metal supports with threaded holes	For solar panel assembly
Threaded screws	For solar panel assembly
Nuts	For solar panel assembly
Screwdrivers	To fix the screws
Red wire	For electrical connection
Black wire	For electrical connection
Multimeter	To do direct measurements
Connectors	To connect components
Welder	To fix connectors and wires
Welding wire	To perform welding

Heat shrinkable tubing	To protect welded wires
Crimper	To crimp connector and wire
Jump wires	To interconnect components
Kapton tape	To protect exposed connections
Scissors	To cut the Kapton tape
Support rod	To support the solar panel
USB-A/USB-B cable	To connect the PC to the Arduino Uno board
Anti-static mat	To protect components from ESD

Table 4.11: *GSE required in the illumination test with incandescent lamp*

The illumination test with incandescent lamp setup is similar to the previous test setup, except that the solar panel shall be exposed to the incandescent lamp.

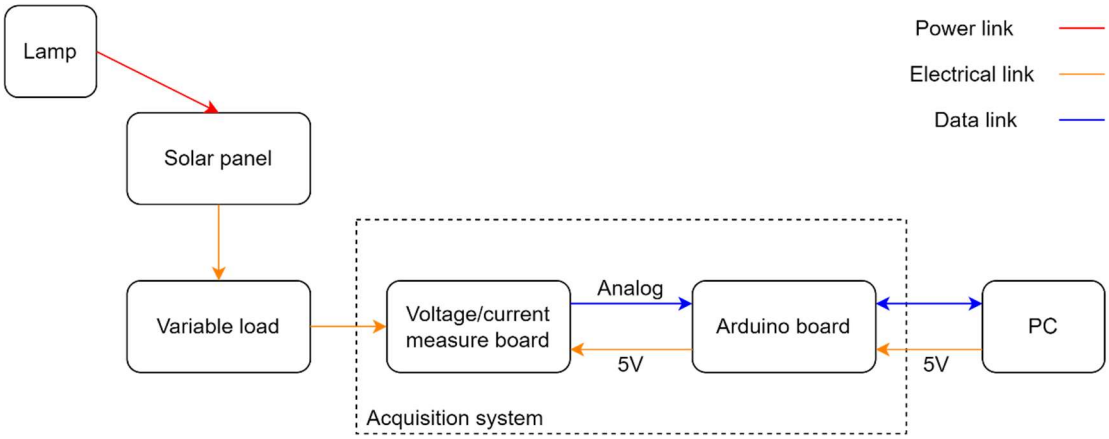

Figure 4.17: *Block scheme of the illumination test with incandescent lamp*

4.5.3 Test execution

The solar panel has been placed on a support rod to guarantee a 90° inclination relative to the horizontal plane. The incandescent lamp, with a power output of 1250 W, has been initially positionated 50 cm away from the solar panel. Then, the open-circuit voltage has been measured through a multimeter before the test began. The Arduino script has been run on the PC, starting to acquire data, while the voltage/current measure board wire has been fixed for about 10 seconds at each load value described in Table 4.8, thus ensuring at least 4 data acquisitions on average per load.

A second test execution has been performed after the lamp had been moved to a 35 cm distance from the solar panel.

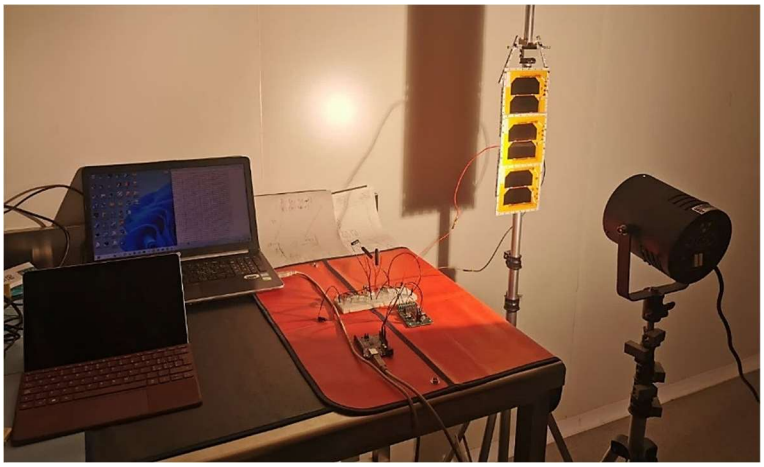

Figure 4.18: *Illumination test execution with the incandescent lamp*

4.5.4 Test result

The illumination tests with incandescent lamp at different distance from the solar panel resulted in the I-V and the P-V curves. The maximum power P_{max} has been identified on the P-V curve and plotted on the I-V curve, identifying the MPP for each plot, and the values are shown in the table below, in which the open circuit voltage has been also reported.

$\boldsymbol{P_{max}}$	$\boldsymbol{0.5\ W}$
$\boldsymbol{I_{mp}}$	$42\ mA$
$\boldsymbol{V_{mp}}$	$11.99\ V$
$\boldsymbol{V_{oc}}$	$14.11\ V$

Table 4.12: *Characteristic points from illumination test with lamp (50 cm)*

$\boldsymbol{P_{max}}$	$\boldsymbol{0.91\ W}$
$\boldsymbol{I_{mp}}$	$74\ mA$
$\boldsymbol{V_{mp}}$	$12.22\ V$
$\boldsymbol{V_{oc}}$	$14.5\ V$

Table 4.13: *Characteristic points from illumination test with lamp (35 cm)*

As Figure 4.19 and Figure 4.20 show, the initial slope of the I-V curve is even higher than in the illumination test with direct sunlight, especially for lower resistor values. Indeed, the current jumps are higher in the first area of the curve, so an increase in the number of low resistors to be used would have helped to decrease the current jumps. Again, no step behaviours due to shading and mismatch losses are observed. Furthermore, Table 4.12 and Table 4.13 show that at a shorter distance from the lamp, the solar panel increases its performance, and in particular an $82\ \%$ increase in maximum power is achieved.

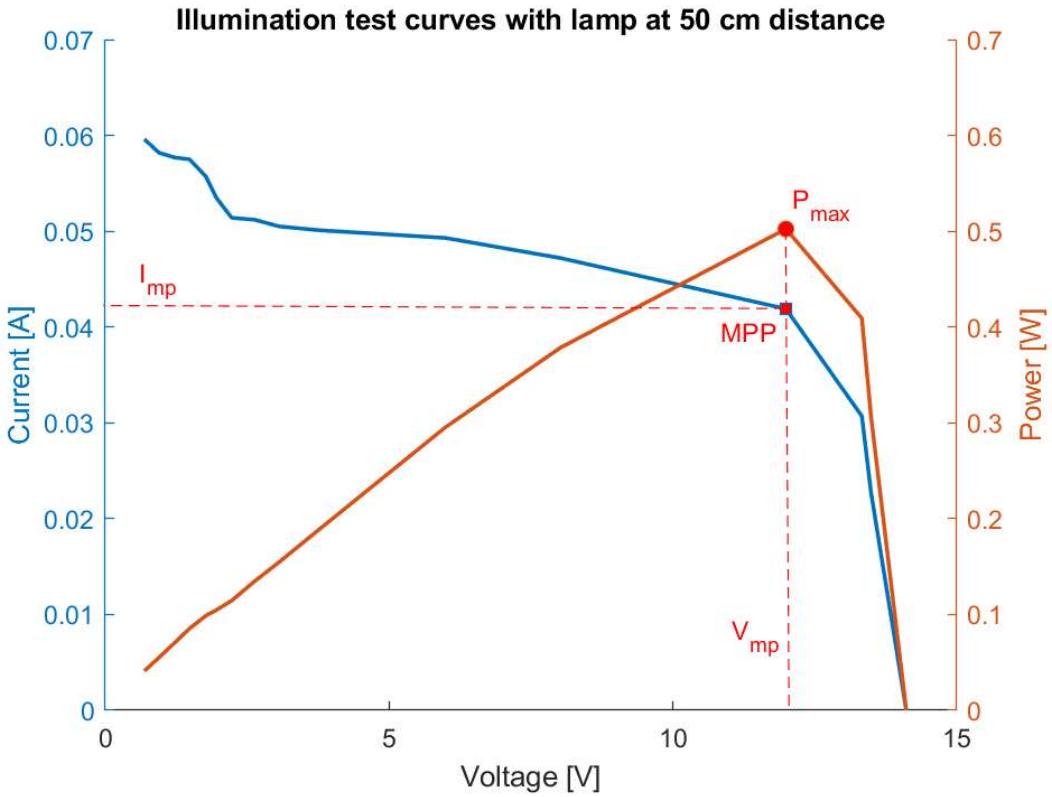

Figure 4.19: *I-V and P-V curves of the illumination test with incandescent lamp (50 cm)*

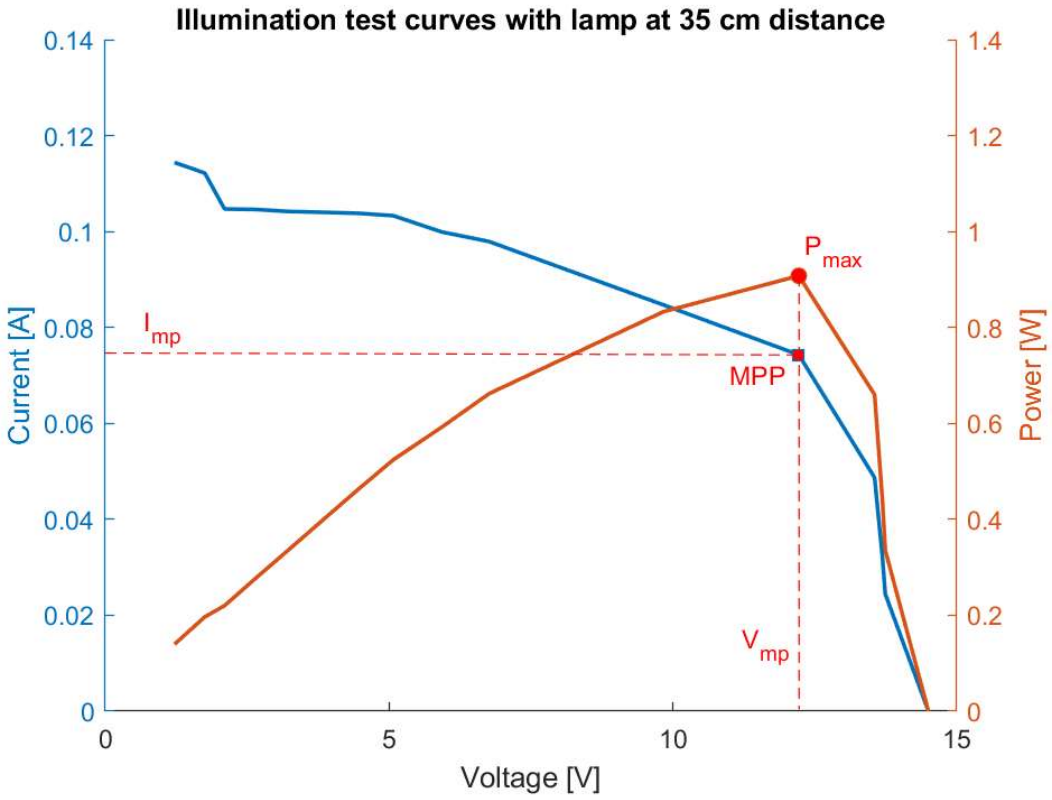

Figure 4.20: *I-V and P-V curves of the illumination test with incandescent lamp (35 cm)*

4.6 Sun Simulation Test

4.6.1 Test objective

The objectives of the sun simulation test aims to verify:

- EPS board telemetry acquisition;
- Battery pack charging;
- Battery pack discharging;
- Solar panel power providing;
- EPS performance in orbit simulation.

What to verify	How to verify	Requirements ID to be verified
EPS board data acquisition	Data evaluation	FUN-125, FUN-192, FUN-195
EPS board power regulation	Data evaluation, direct measurement with GSE	FUN-100, FUN-170, FUN-173, FUN-182, FUN-183
EPS board power distribution	Data evaluation, direct measurement with GSE	FUN-100, FUN-150, FUN-155, INT-055
Battery charging	Data evaluation	FUN-120, FUN-145, FUN-173, INT-055
Battery discharging	Data evaluation	FUN-100, FUN-135, FUN-140, FUN-145, FUN-153

Table 4.14: *EPS requirements to be verified in the sun simulation test*

4.6.2 Test setup

The equipment employed for the setup of the sun simulation test are:

- Battery pack, described in Section 3.2.2;
- EPS board, described in Section 3.2.3;
- Power bench;
- Arduino Nano board;
- Breadboard;
- Resistor;
- PC.

GSE used in the test are described in Table 4.15.

EQUIPMENT	Comments
Multimeter	To do direct measurements
Connectors	To connect components
Welder	To fix connectors and wires
Welding wire	To perform welding
Heat shrinkable tubing	To protect welded wires
Crimper	To crimp connector and wire
Crocodile clips	To connect the power bench
Jump wires	To interconnect components
Kapton tape	To protect exposed connections
Scissors	To cut the Kapton tape
NTC thermistor	To measure battery pack temperature
USB-A/Mini-B cable	To connect the PC to the Arduino Nano board
RS-232 crossover cable	To connect the PC to the power bench
RS-232/USB-A cable	To connect the PC to the power bench
Anti-static mat	To protect components from ESD

Table 4.15: *GSE required in the sun simulation test*

The sun simulation test setup requires the power bench to be connected to the EPS board in both solar panel access ports, through crocodile clips connected to channel 1 and channel 2 of the power bench. The constant load consists of a resistor equipped with a connector compatible to the load access port of the EPS board. The battery pack shall be connected to the EPS board through the first battery pack access port. The Arduino Nano board is the interface between the EPS board and the PC, and allows a SPI communication line via jump wires. The PC communicates with the Arduino board through the USB-A/Mini-B cable, connected to the USB0 port of the PC. Via the same cable, the PC supplies 5 V to the Arduino board. The PC communicates also with the power bench through the RS-232 crossover cable combined with the RS-232/USB-A cable, connected to the USB1 port of the PC.

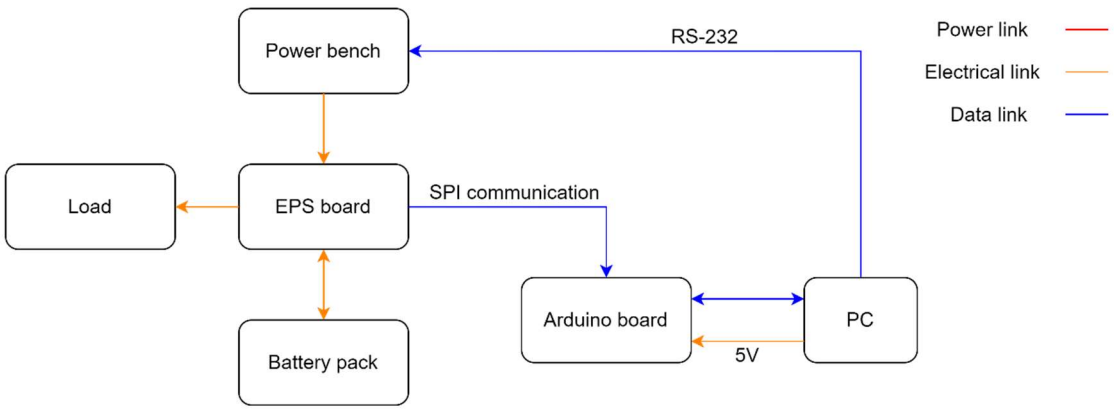

Figure 4.21: *Block scheme of the sun simulation test*

4.6.3 Test execution

The sun simulation test execution has been performed by considering a resistive load that simulates the most power demanding operative mode, as reported in the power budget described in Section 2.4.2.

The 67 Ω resistor has been selected as the resistive load for the sun simulation test execution, because it represents the closest available resistor value to the worst case considered. The calculations performed in order to select the resistor value are described in Appendix E.

Before starting the test, the overcurrent protection limit in channels 1 and 2 of the power bench has been set to $13.5\ V$, as for the battery charge test since that limit is required by the battery. Then, the Arduino sketch has been compiled and the resulting executable file has been run through the minicom terminal on the PC. The Arduino board started reading values from the ADC on the EPS board every second and these values have been displayed on the PC's terminal. Afterwards, another minicom terminal has been open in order to compile the C code destinated to perform the communication between the PC and the power bench. Before running the executable file obtained, the load, the battery pack and the NTC thermistor have been connected to the EPS board. Finally, the power bench has been start update their values on the two channels employed and also the terminals on the PC printed the data acquired every second.

An anomaly detected concerned the resistor, which started to overheat immediately after the start of the test. To remedy this problem, a cold aluminium plate has been placed under the resistor and a heat sink compound has been applied between the resistor and the plate.

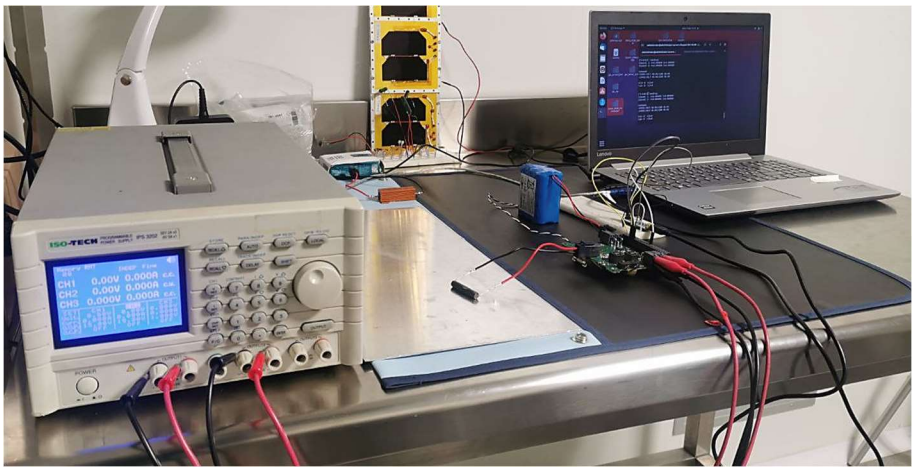

Figure 4.22: Sun simulation test execution

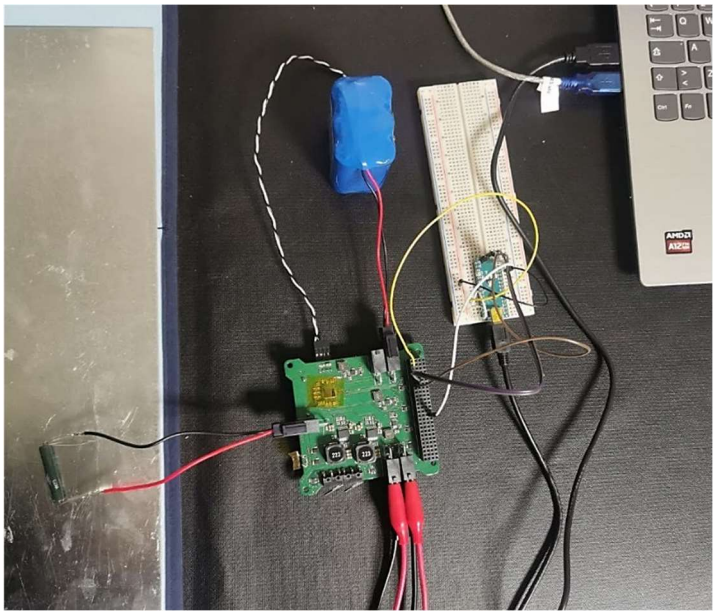

Figure 4.23: *Zoom on interfaces during the sun simulation test execution*

4.6.4 Test result

The sun simulation test has been performed in about 8 and a half hours, simulating five orbits. Figure 4.24 shows that each orbit has a battery charging phase, representing the sunlight period, in which the battery voltage has an overall increasing trend, and a battery discharging phase, representing the eclipse period, in which the battery voltage decreases until it reaches its lowest value. Furthermore, numerous voltage and current fluctuations are evident in the battery charging phase, due to the updating of input values to the power bench every second. On the other hand, the battery discharging phase has zero voltage and current supplied by the power bench, therefore the trends in battery discharge current and voltage are free of fluctuations. In addition, the lowest voltage reached by the battery at the end of each orbit, which represents the battery's State Of Charge (SOC), increases as more orbits are performed, as shown in Table 4.16. This is mainly due to the gradual increase in sunlight periods, which allow the battery to be charged a little more each time, and the eclipse periods are slightly reduced, so that the battery is discharged a little less.

	SUNLIGHT PERIOD	ECLIPSE PERIOD	LOWEST BATTERY VOLTAGE	SOC
ORBIT 1	93.73 min	10.52 min	11.78 V	82.13 %
ORBIT 2	94.45 min	9.65 min	11.79 V	82.39 %
ORBIT 3	95.15 min	8.72 min	11.79 V	82.46 %
ORBIT 4	95.98 min	7.62 min	11.81 V	82.87 %
ORBIT 5	97.06 min	6.35 min	11.82 V	83.09 %

Table 4.16: *Lowest battery voltage trend in 5 orbits*

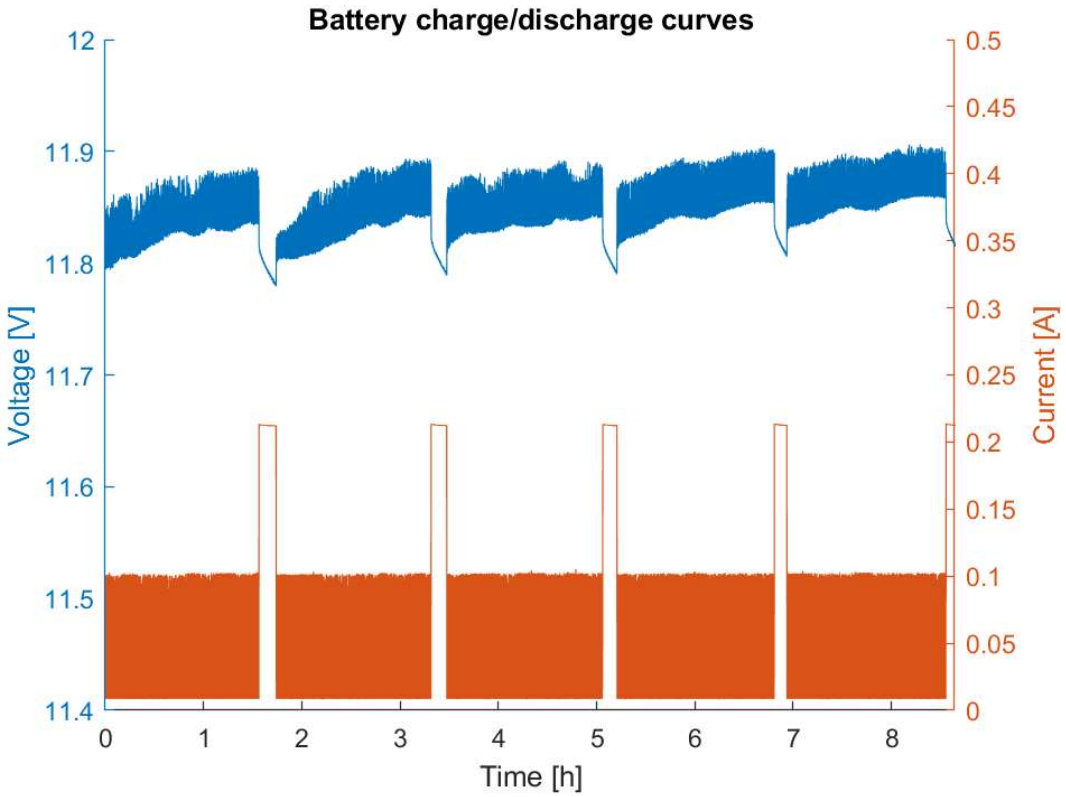

Figure 4.24: *Sun simulation test results*

The temperature trend measured on the battery throughout the sun simulation test is increasing, reaching a maximum value of $29.65\ °C$.

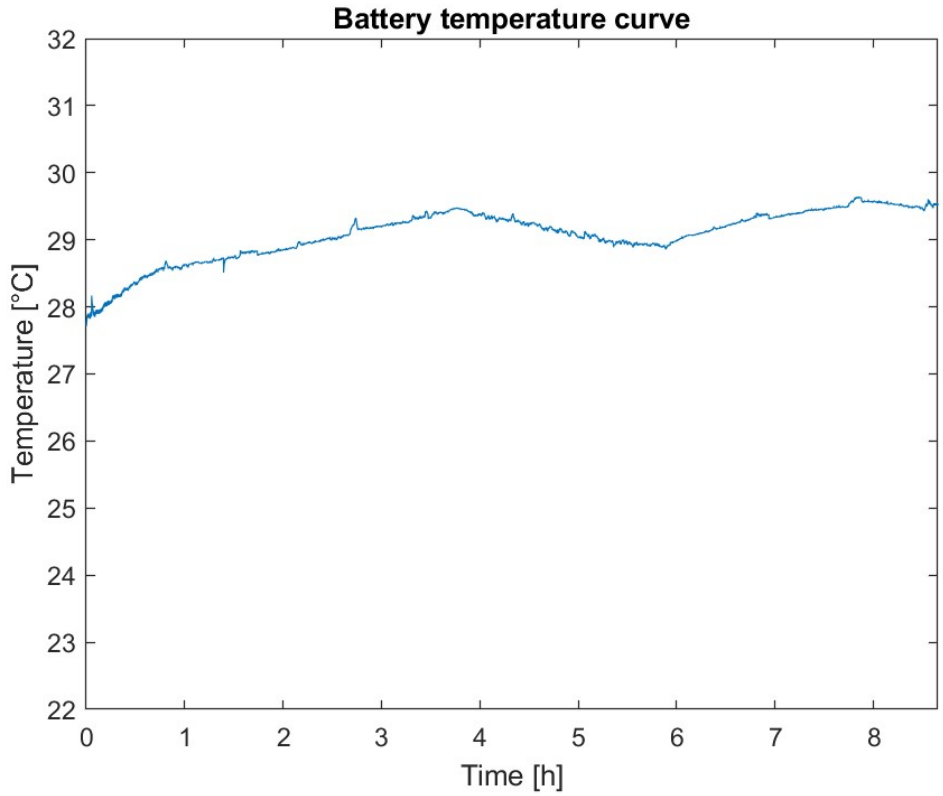

Figure 4.25: *Battery temperature during sun simulation test*

4.7 EPS Integration Test

4.7.1 Test objective

The objectives of the EPS integration test aims to verify:

- EPS board telemetry acquisition;
- Battery pack charging;
- Battery pack discharging;
- Solar panel power providing;
- EPS integration performance.

What to verify	How to verify	Requirements ID to be verified
EPS board data acquisition	Data evaluation	FUN-125, FUN-192, FUN-195
EPS board power regulation	Data evaluation, direct measurement with GSE	FUN-100, FUN-170, FUN-173, FUN-182, FUN-183
EPS board power distribution	Data evaluation, direct measurement with GSE	FUN-100, FUN-150, FUN-155, INT-055
Battery charging	Data evaluation	FUN-120, FUN-145, FUN-173, INT-055
Battery discharging	Data evaluation	FUN-100, FUN-135, FUN-140, FUN-145, FUN-153
Solar panel power generation	Data evaluation, direct measurement with GSE	FUN-100, FUN-110, FUN-145, FUN-153, INT-052

Table 4.17: *EPS requirements to be verified in the EPS integration test*

4.7.2 Test setup

The equipment employed for the setup of the EPS integration test are:

- 3U solar panel, described in Section 3.2.1;
- Battery pack, described in Section 3.2.2;
- EPS board, described in Section 3.2.3;
- Arduino Nano board;
- Breadboard;
- Resistor;
- PC.

GSE are described in Table 4.18.

EQUIPMENT	Comments
Metal supports with threaded holes	For solar panel assembly
Threaded screws	For solar panel assembly
Nuts	For solar panel assembly
Screwdrivers	To fix the screws
Red wire	For electrical connection
Black wire	For electrical connection
Multimeter	To do direct measurements
Connectors	To connect components
Welder	To fix connectors and wires
Welding wire	To perform welding
Heat shrinkable tubing	To protect welded wires
Crimper	To crimp connector and wire
Jump wires	To interconnect components
Kapton tape	To protect exposed connections
Scissors	To cut the Kapton tape
NTC thermistor	To measure solar panel temperature
USB-A/Mini-B cable	To connect the PC to the Arduino Nano board
Anti-static mat	To protect components from ESD

Table 4.18: *GSE required in the EPS integration test*

The EPS integration test setup requires the solar panel to be exposed to the Sun. The solar panel shall be connected to the EPS board in the first solar panel access port through a compatible connector. The battery pack shall be connected to the EPS board through the first battery pack access port. The constant load consists of a resistor equipped with a connector compatible with the load access port of the EPS board. The Arduino Nano board is the interface between the EPS board and the PC, and allows a SPI communication line via jump wires. The PC communicates with the Arduino board through the USB-A/Mini-B cable, connected to the USB0 port of the PC. Via the same cable, the PC supplies 5 V to the Arduino board.

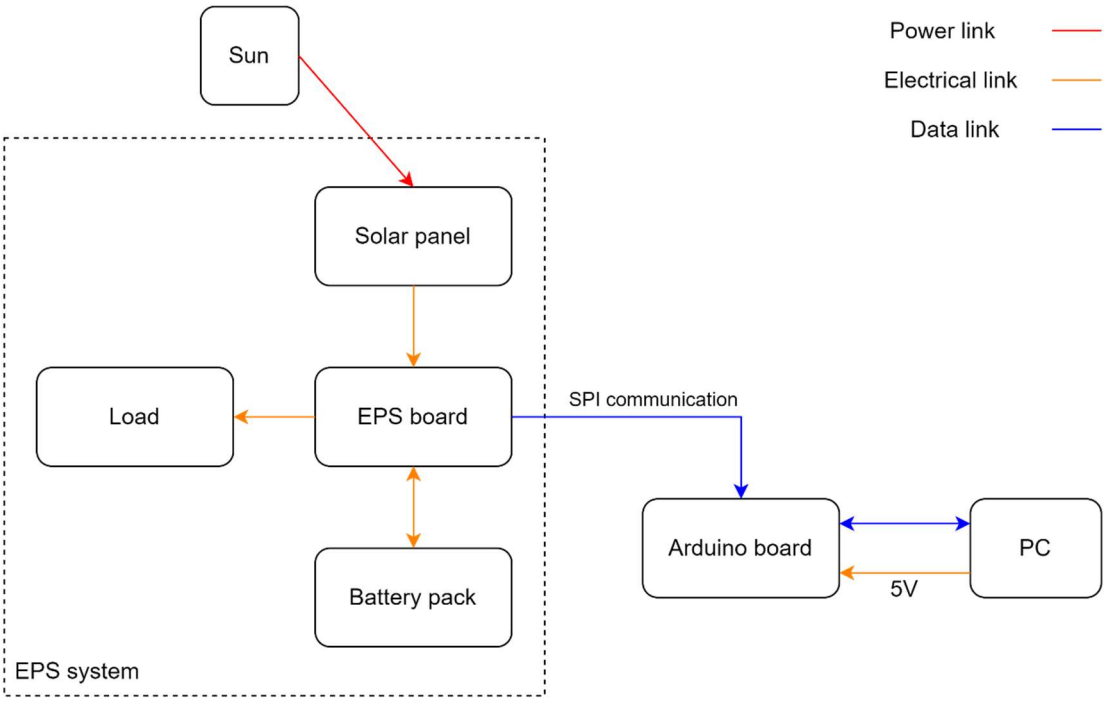

Figure 4.26: *Block scheme of the EPS integration test*

4.7.3 Test execution

The EPS integration test execution has been performed by considering the same resistive load used in the sun simulation test. Same considerations and calculations are described in Appendix E.

The solar panel has been tilted by about 85° in order to generate the maximum power. The solar panel, the load and the NTC thermistor have been connected to the EPS board. Afterwards, the Arduino sketch has been compiled and the resulting executable file has been run through the minicom terminal on the PC. The Arduino board started reading values from the ADC on the EPS board every second. Finally, the battery pack has been connected to the EPS board and the values continue to be read by the PC's terminal.

After about 56 minutes from the start of the test, the solar panel and the NTC thermistor have been disconnected form the EPS board in order to simulate the end of the sunlight period and the start of the eclipse period, as in orbit conditions. About 36 minutes later, the battery pack has been disconnected too and data acquisition has been stopped.

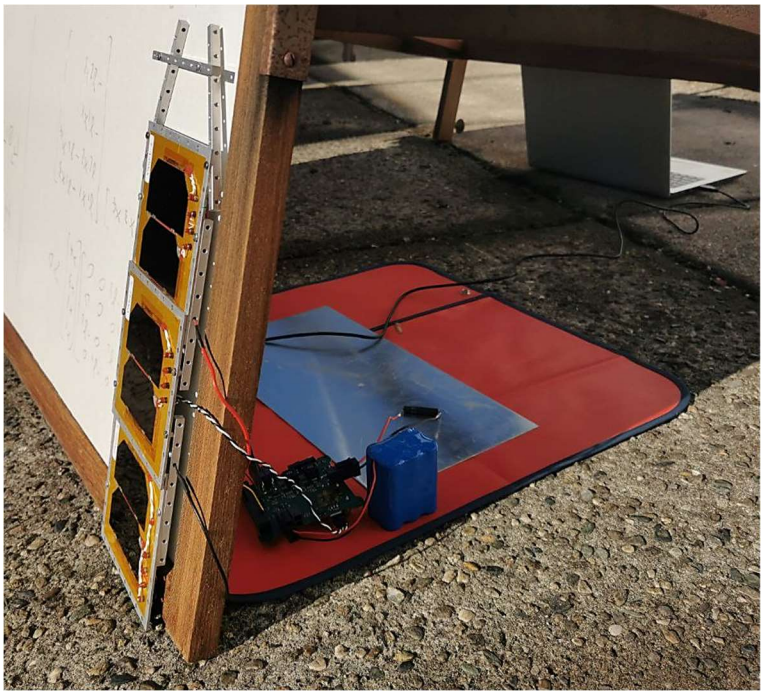

Figure 4.27: *EPS integration test execution*

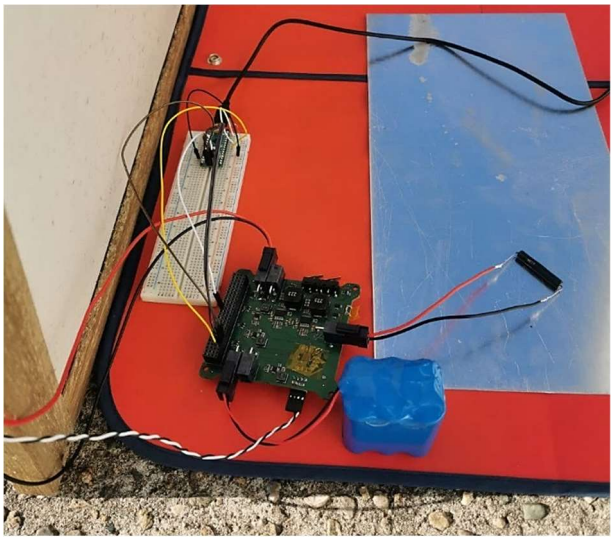

Figure 4.28: *Zoom on interfaces during the EPS integration test execution*

4.7.4 Test result

The EPS integration test has been performed in about 92 minutes, of which approximately 56 minutes represented the sunlight period. The solar panel charged the battery, which increased its voltage as shown in Figure 4.29. The discontinuity in the graph represents the end of the sunlight period and the beginning of the eclipse period, during which the battery has been discharged, leading to a gradual decrease in its voltage. Overall, the battery has discharged by about $8\,\%$, as it started the test with a $SOC = 51.05\,\%$ and ended it with a $SOC = 42.63\,\%$.

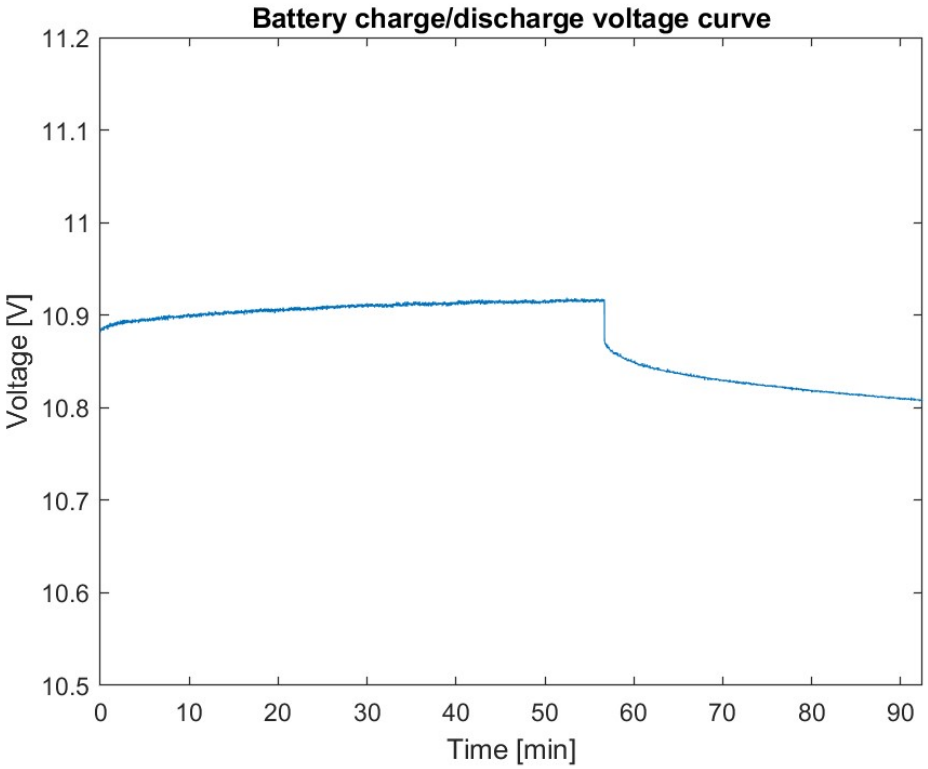

Figure 4.29: *EPS integration test results*

In addition, the temperature of the solar panel has been measured during its operational period, thus in the first 56 minutes, when it reached a peak of $41.72\ °C$.

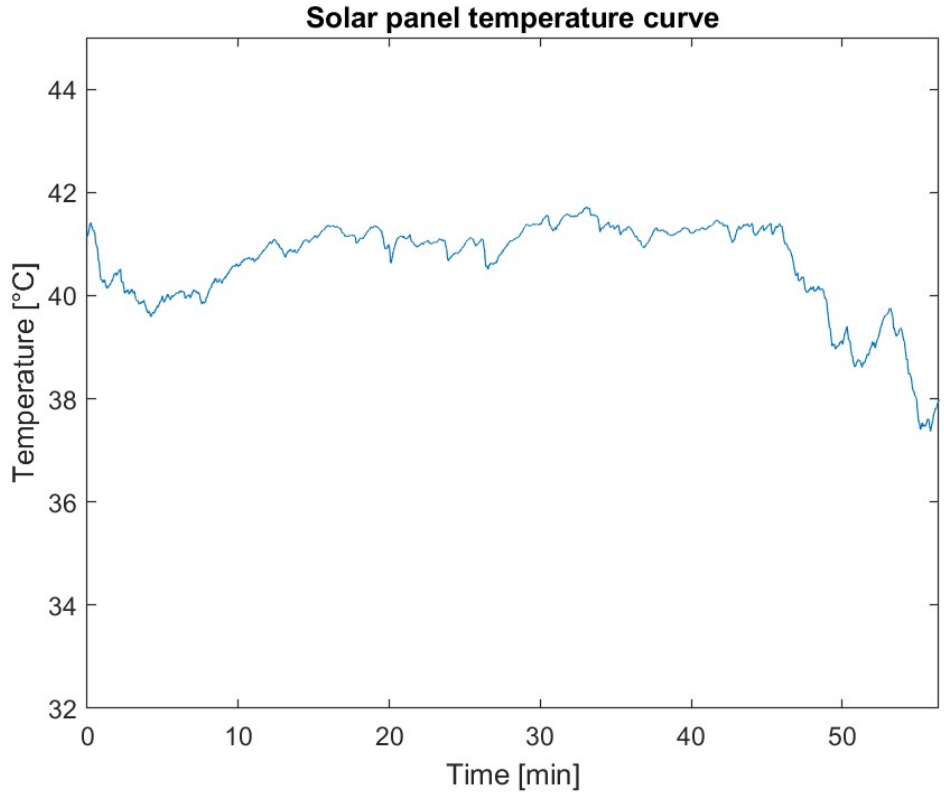

Figure 4.30: *Solar panel temperature during EPS integration test*

5 Conclusions

The main objective of this thesis has been the delevopment of an Electrical Power System for a 3U educational CubeSat, starting with a functional analysis of the system in order to understand its functionality in CubeSat applications. The study of the state of the art has been fundamental to developing the system and figuring out the optimal configuration for the SILVA mission. Further to the study of the functional analysis and preliminary configuration, the EPS sizing has been an important step to better define the system and understand its features in terms of performance. The identification of the flight model led to the start of the procurement phase, as the Starbuck-Nano will be the board predestined to reach space, while solar cells and battery will have to be procured in the future. Therefore, the work carried out in this thesis could be a good point to continue the realisation of the flight model.

However, an Electrical and Functional Model has been developed in order to perform some verification test and verify the requirements defined during the system design phases. The execution of six different tests gave very good results, which confirm the elaborated design. For example, in the battery discharge test, the battery has been characterised and the complete discharge allowed the SOC of the battery to be defined and the battery's behaviour and electrical characteristics during discharge to be analysed. In addition, this test has also been crucial for the comprehension of the other test results, such as the sun simulation test and the EPS integration test, where the SOC of the battery has been analysed to understand the behaviour of the EPS during a simulated orbit period. The battery charge test provides insight into the behaviour of the battery during charging, while the illumination tests both under the sun, to simulate direct sunlight conditions in orbit, and with the lamp, to simulate the sun, have been fundamental in characterising the solar panel, and in understanding the differences between the two tests. Moreover, the solar panel has been assembled for the first time in the STARlab, so it was essential to characterise it to understand how much power it could provide and how it is affected by the load absorbing power. The sun simulation test clearly demonstrated the adequacy of the battery's and board's behaviour in a simulated orbital condition, giving a very positive result. The integration test has been the last test in which all components of the EPS has been integrated and tested together. The orbit simulation clearly verify some requirements, such as the ability of the solar panels to generate power and distribute it to the load and at the same time charge the battery.

A limitation encountered during this thesis work is related to the EFM of the EPS board, as the board does not have a dedicated ADC channel for reading the solar panel voltage, which represented one of the most challenging issues of the thesis work. For this reason, a voltage/current measure board has been developed. A further problem concerned the selection of resistors, as the choice was limited to those available in the STARlab. Lastly, the conversion of data from raw to real constituted a further limitation, because the code was

not optimised and some problem occurred in the conversion of the battery charging current, which turned out to have very low values that were clearly unrealistic.

Considering the work done and the limitations found in this thesis, some recommendations are advised. A few suggestions for the future development of the EPS are the improvement of the software employed, such as the optimisation of the Python code for data conversion and the C code used in the sun simulation test. In addition, it would certainly be interesting to investigate how the EPS could be integrated with other subsystems, for example initially replacing the Arduino with the OBC for data acquisition. Subsequently, integration with other subsystems could also be implemented to simulate the potential load of the mission, thus removing the problems encountered in using resistors to simulate the resistive load of the satellite. Another future work could be the completion of battery charging, as only the constant current (CC) charging phase has been characterised, while the constant voltage (CV) charging phase has not yet been. An improvement of the resistor range, particularly for low resistors, could naturally be useful to better characterise the I-V and P-V curves of the solar panel. Furthermore, the incandescent lamp could be used at a shorter distance than in the tests performed and a solution could be developed to channelling the light into the six solar cells of the panel. Finally, an increase in the number of solar cells employed can be considered, for example by occupying the upper (*z+*) face of the CubeSat that has been empty until now.

In conclusion, the development of the EPS conducted in this thesis may represent a good starting point for continuing the SILVA mission design and further development of the Electrical Power System.

Appendixes

Appendix A

Table A - 1: *Solar cells characteristics collection*

Company	Cell Name	Cell Area $[cm^2]$	BOL Efficiency	$V_{oc}\ [V]$	$V_{mp}\ [V]$	$I_{sc}\ \left[\frac{mA}{cm^2}\right]$	$I_{mp}\ \left[\frac{mA}{cm^2}\right]$
AZUR SPACE [11]	S 32	23.61	16.9 %	0.628	0.528	45.8	43.4
	TJ 3G28C	30.18	28 %	2.667	2.371	16.77	16.14
	TJ 3G30C	30.18	29.5 %	2.7	2.411	17.24	16.7
		26.51					
	QJ 4G32C	30.18	31.8 %	3.451	3.025	15.16	14.36
Rocket Lab [12]	ZTJ	-	29.5 %	2.726	2.41	17.4	16.5
	ZTJ+	-	29.4 %	2.69	2.39	17.11	16.65
	ZTJ-Ω	-	30.2 %	2.73	2.43	17.41	16.8
	Z4J	-	30 %	3.95	3.54	12	11.5
	IMM-α	-	32 %	4.78	4.28	10.66	10.12
Spectrolab [13]	UTJ	26.6	28.3 %	2.66	2.35	17.14	16.38
	XTJ	26.6	29.5 %	2.633	2.348	17.76	17.02
	XTJ Prime	26	30.7 %	2.72	2.406	18	17.5
		27					
	XTE-SF	27	32.2 %	2.75	2.435	18.6	17.9
CESI [9]	CTJ-LC	26.5	28 %	2.62	2.32	17.25	16.45
		27.5					
		30.15					
	CTJ-30	26.5	29.5 %	2.6	2.32	17.85	17.17
		27.5					
		30.15					
	CTJ-30 Thin	26.5	29 %	2.61	2.31	17.85	17.13
		27.5					
		30.15					

Table A - 2: *3U solar panel characteristics collection*

Company	Product	Cell Type	Specific Power $[W/kg]$	Peak BOL Power $[W]$
AAC Clyde Space [10]	PHOTON	XTJ Prime	67	9
DHV Technologies [14]	SPC-CS30	-	64	8.48
ISISPACE [15]	-	TJ 3G30C	46	6.9
EnduroSat [16]	-	-	66	8.4

Table A - 3: *Batteries characteristics collection*

Company	Product	Cell Type	Specific Energy $[Wh/kg]$	Typical Capacity $[Wh]$	Max Discharge Rate $[A]$
AAC Clyde Space [10]	OPTIMUS-30	LiPo	112	30	1.95
	OPTIMUS-40		119	40	2.6
GomSpace [17]	NanoPower BP4 (2P-2S)	Li-ion	149.2	38.5	2.5
	NanoPower BPX (2S-4P)		150	75	
	NanoPower BPX (4S-2P)				
Ibeos [18]	B14-M45	Li-ion	120	45	6.5
Saft [19]	4S-1P VES16	Li-ion	91	64	-
EXA [20]	BA01/S	LiPo	193	22.2	-
	BA01/D		207	44.4	-
NRG srl [21]	Li-NMC	LiPo	180	24	-

Table A - 4: *PCDU characteristics collection*

Company	Product	Peak Output Power $[W]$	Input Voltages $[V]$	Output Voltages $[V]$	Max Efficiency
AAC Clyde Space [10]	STARBUCK-NANO	-	3 - 30	3.3 / 5 / 12 / Unreg Batt	92 %
DHV Technologies [14]	NanoEPS	-	3 - 28	3.3 / 5 / 12 / Unreg Batt	93 %
EnduroSat [16]	EPS I	10 - 20	0 - 5.5	3.3 / 5 / Unreg Batt	86 %
	EPS I Plus	30			
Ibeos [18]	E14-150	150	18 - 42	3.3 / 5 / 12 / Unreg Batt	95 %
NanoAvionics [22]	CubeSat EPS	100	2.6 - 18	3.3 / 5 / 3-12	96 %

Appendix B

Table B - 1: *SILVA Mission Scenarios*

Mission Sub-phase	Mission Scenario
Launch	This phase covers all the activities to be performed in order to support the launch and the ascent phase towards the parking orbit (ConOps1) or the ISS (ConOps2).
Deployment ConOps1	This phase covers all the activities to be performed to support the separation of the spacecrafts from the dispenser.
Deployment ConOps2	This phase covers all the activities to be performed in order to deploy the CubeSat into orbit as a separate artificial satellite by the use of Nanoracks CubeSat Deployer (NRCSD).
EOP	This phase covers all the activities to be performed to check and activate subsystems and payload. The satellite may have some rotations induced by the deployment mechanism during orbit insertion and the detumbling is performed. Once the satellite is stable, other actuators can take over for fine attitude control required for nominal operation. During this commissioning phase, subsystems are tested, and housekeeping data are sent to the ground to verify the presence of anomalies and health's state of satellite during subsystem checkouts. The LEOP finalizes with the payload commissioning: ADCS shall ensure the correct pointing of the payload and it is necessary to perform tests to check for the payload function, power consumption and transmission of science data for safe nominal operations.
Science Operations	This phase covers all the activities to be performed to achieve the mission scientific objectives. The payload takes pictures of the target to monitor large green areas providing specific data on their health.
Technology Demonstration	This phase covers all the activities to be performed to achieve the mission technology objectives. The payload performs the Super Resolution Reconstruction (SRR) algorithms to ensure on-board data processing. The UHF-board transmits housekeeping telemetry packets every 30 seconds and S-board transmits mission data. Recharging of batteries is also planned during this phase.
Disposal	This phase covers all the activities to be performed in order to avoid formation of spatial debris. A natural disposal is seen as the most effective method of meeting orbital debris mitigation standards. During passivation, all latent energy reservoirs of satellite are depleted to prevent an accidental post-mission explosion. After passivation, since the casualty on ground during the re-entry is less than 10^{-4}, an uncontrolled re-entry is performed.

Table B - 2: *SILVA Operative Modes*

Operative Mode	Application Criteria	Description	Phase
Dormant Mode (All subsystems and payload are turned off)	CubeSat is in the launcher.	CubeSat is not powered. At least two switches open the powering circuits. All subsystems are off. Batteries are halfway charged.	Launch and Deployment
Detumbling Mode (CubeSat detumbling)	CubeSat has been just ejected from the launcher.	EPS is turned on by closing the switches. OBC is turned on. ADCS is turned on. ComSys is off. Payload is off. Batteries provide the required power. ADCS performs detumbling. ADCS requires most of the power.	EOP
Commissioning Mode (Functional test of subsystems and payload is performed)	Detumbling is over and CubeSat attitude has been quite stabilized.	OBC checks subsystems' critical parameters. OBC runs health algorithms. OBC checks subsystems parameters. Solar Panels start generating power. ADCS performs nadir pointing. Antennas are deployed. ComSys is turned on. ComSys starts transmitting housekeeping telemetry. Payload is turned on. Payload is checked. Payload is calibrated (if required).	EOP
Basic Mode (CubeSat is in a stationary mode)	No commands are issued. Subsystems' parameters are in nominal ranges. CubeSat is in a generic, uninteresting position in orbit.	EPS is on. OBC is on. ADCS is on. ComSys is on (S board is in stand-by - reception only status, UHF board transmits housekeeping telemetry packets every 30 seconds). Payload elaborates images. Payload performs super reconstruction algorithm.	Technology Demonstration
Mission Mode (CubeSat is in its mode of operation)	Command is issued. CubeSat is above mission targets.	EPS is on. OBC is on. ADCS is on. ADCS guarantees nadir pointing.	Science Operations

		ComSys is on. S board is in stand-by - reception only status. UHF board transmits housekeeping telemetry packets every 30 seconds). Payload takes pictures of the target.	
Transmission Mode (Communication with ground is established)	Command is issued. CubeSat is in line of sight with selected ground stations.	EPS is on. OBC is on. ADCS is on. ADCS guarantees nadir pointing. ComSys is on. S board transmits mission data. UHF board transmits telemetry housekeeping data every 30 s. Payload is in stand by status.	Technology Demonstration
Safe Mode (In case of failure of subsystems and/or payload)	Off nominal conditions are met.	Subsystems' activities are reduced to the minimum. Payload stops executing operations. OBC checks subsystems' parameters. OBC runs health algorithms. OBC performs recovery actions.	All Phases
Passivated Mode (All subsystems and payloads are off)	Mission Operations are over.	OBC is switched off. Batteries are discharged. All subsystems and payloads are off	Disposal

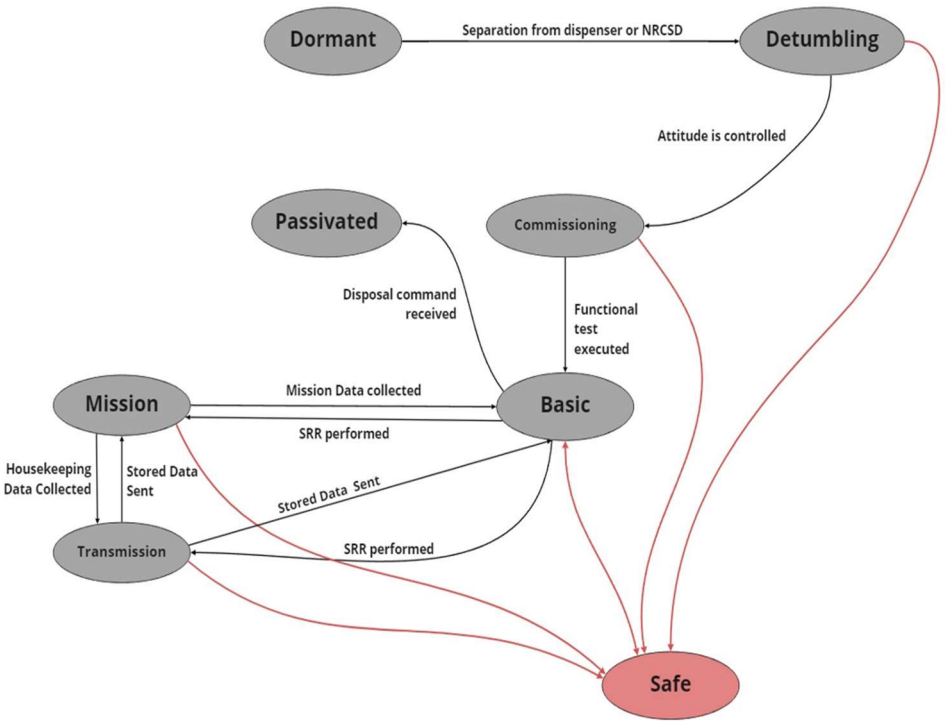

Figure B - 1: *Transitions between SILVA operative modes*

Appendix C

```
%% EPS sizing
clear all
close all
clc

%% Mission parameters
Sat_l=5; %Satellite life [years]

%% Orbital parameters
h=[400 700]; %Orbit altitude [km]
G=6.67*(10^-11); %Gravitational constant [Nm^2/kg^2]
M_earth=5.972*(10^24); %Earth mass [kg]
R_earth=6371; %Earth radius [km]
T_orbit=2*pi*sqrt((((R_earth+h).*1000).^3)./(G*M_earth)); %Orbital
period [s]
i=[51.6 97]; %Orbit inclination [°]
Gamma=0; %True ecliptic solar longitude [°]
RAAN=0; %Longitude of the ascending node [°]
epsilon=23.45; %Earth's axial obliquity [°]
beta=[0 0]; %Worst case orbital beta angle [°]

for j=1:2
    rho(j)=asind(R_earth./(R_earth+h(j))); %Earth angular radius [°]
    phi(j)=2.*acosd(cosd(rho(j))./cosd(beta(j))); %[°]
    T_e(j)=T_orbit(j).*phi(j)/360; %Eclipse period per orbit [s]
    T_d(j)=T_orbit(j)-T_e(j); %Daylight period per orbit [s]
end

%% Power budget

Mrg=[1.05 1.1 1.2]; %Margins to apply in the power budget

% Index 1 is Detumbling mode
% Index 2 is Commissioning mode
% Index 3 is Basic mode
% Index 4 is Mission mode
% Index 5 is Transmission mode
% Index 6 is Safe mode

time_op=30*[1 1 1 1 1 1]; %Operative modes duration [min]
Payload_power=Mrg(3)*[0 5 5 5 0 0]; %Payload power consumption [W]
ADCS_power=Mrg(3)*[0.3 1.09 0.54 1.26 1.09 0.18]; %ADCS power
consumption [W]
ComSys_power=Mrg(3)*[0 4.29 3.71 3.71 4.29 0]; %ComSys power
consumption [W]
```

```
OBC_power=Mrg(3)*[1.2 1.2 1.2 1.2 1.2 1.2]; %OBC power consumption
[W]
EPS_power=Mrg(2)*[0.3 0.3 0.3 0.3 0.3 0.2]; %EPS power consumption
[W]

for i=1:length(time_op)
      P_sc(i)=Payload_power(i)+ADCS_power(i)+ComSys_power(i)+OBC_powe
      r(i)+EPS_power(i);
end

% Plot Power-Time
figure()
hold on
grid on
rectangle('Position',[0 0 time_op(1) P_sc(1)],'FaceColor','#0072BD')
det_line=line(NaN,NaN,'LineWidth',1.5,'LineStyle','-
','Color','#0072BD');
rectangle('Position',[time_op(1) 0 time_op(2)
P_sc(2)],'FaceColor','#D95319')
com_line=line(NaN,NaN,'LineWidth',1.5,'LineStyle','-
','Color','#D95319');
rectangle('Position',[time_op(1)+time_op(2) 0 time_op(3)
P_sc(3)],'FaceColor','#EDB120')
basic_line=line(NaN,NaN,'LineWidth',1.5,'LineStyle','-
','Color','#EDB120');
rectangle('Position',[time_op(1)+time_op(2)+time_op(3) 0 time_op(4)
P_sc(4)],'FaceColor','#7E2F8E')
mission_line=line(NaN,NaN,'LineWidth',1.5,'LineStyle','-
','Color','#7E2F8E');
rectangle('Position',[time_op(1)+time_op(2)+time_op(3)+time_op(4) 0
time_op(5) P_sc(5)],'FaceColor','#77AC30')
transmission_line=line(NaN,NaN,'LineWidth',1.5,'LineStyle','-
','Color','#77AC30');
rectangle('Position',[time_op(1)+time_op(2)+time_op(3)+time_op(4)+ti
me_op(5) 0 time_op(6) P_sc(6)],'FaceColor','#A2142F')
safe_line=line(NaN,NaN,'LineWidth',1.5,'LineStyle','-
','Color','#A2142F');
xlabel('Time [min]')
xlim([0 250])
ylabel('Power [W]')
ylim([0 20])
title('Spacecraft power consumption')
legend([det_line,com_line,basic_line,mission_line,transmission_line,
safe_line],'Detumbling mode','Commissioning mode','Basic
mode','Mission mode','Transmission mode','Safe mode')

%% Solar array parameters
P_e=max(P_sc); %Power requirements during eclipse [W]
```

```
P_d=P_e; %Power requirements during daylight [W] (could be different
from P_e)
X_e=0.6; %Path transmission efficiency during eclipse
X_d=0.8; %Path transmission efficiency during daylight
eta_c=0.28; %Ideal solar cells efficiency [%]
Irr=1367; %Incident solar radiation [W/m^2] (if normal to surface of
cells)
I_d=0.77; %Inherent degradation of solar array
theta=23.5; %Sun incidence angle [deg] (worst case by Wertz)
Deg_y=0.005; %Degradation/year (Multijunction 0.5% per year)
eta_P=38; %Solar array power density [W/kg]

%% Battery parameters
DoD=0.4; %Depth of Discharge [%]
N_batteries=2; %Number of batteries
n=0.98; %Transmission efficiency
Disch=0.003; %Self discharge per day [%]
rho_e=125; %Specific energy density [Wh/kg]
V_batt_bus=8.2; %Battery Bus Voltage [V]

%% Calculations
% Solar Array Sizing
P_sa=((P_e.*T_e/X_e)+(P_d.*T_d/X_d))./T_d; %Solar array power [W]
P_o=eta_c*Irr; %Ideal solar cells power output [W/m^2]
P_BOL=P_o*I_d*cosd(theta); %Solar array power per unit area at BOL
[W/m^2]
L_d=(1-Deg_y)^Sat_l; %Life degradation
P_EOL=P_BOL*L_d; %Solar array power per unit area at EOL [W/m^2]
A_sa=P_sa./P_EOL; %Solar array area [m^2]
M_sa=P_sa./eta_P; %Solar array mass [kg]

% Battery Sizing
C_r_W=P_e*(T_e/3600)/(DoD*N_batteries*n); %Battery capacity [W*h]
C_r_A=C_r_W/V_batt_bus; %Batteries capacity [A*h]
M_b=C_r_W/rho_e; %Battery mass [kg]
n_cycles=(Sat_l*365.25*24*60)./(T_orbit/60); %number of charge-
discharge cycles
```

Appendix D

Table D - 1: *Step-by-step procedure for solar panel assembly*

Step n°	Action	Pass/fail criteria	Expected results
0	Solar Panel Assembly		
10	Merging the three solar panels structurally		Get a single solar panel
11	Measuring the three solar panels	Get measurements	Measure length, width, and thickness in cm
12	Overlapping the three solar panels	Get a shorter solar panel	Achieve 30 cm distance from the beginning of the first cell to the end of the last one
13	Place four structural supports at the back of the solar panels		Obtain a balanced solar panel on a surface
14	Screwing screws from the solar panel to the structural supports	Move the solar panel	Getting a solar panel with structural supports fixed
20	Connect the three solar panels in series with red and black cables		Get a higher voltage measurement
30	Measuring the voltage of the solar panel obtained	The voltage must be other than zero	A positive voltage in the solar panel when exposed to a light source
40	Applying connectors to the ends of the cables		
41	Welding the connector to the cable end	Move the connector	
42	Clamp the connector with the gripper	Move the connector	

Appendix E

The selection of the resistive load for the battery discharge test required some analytical calculations in order to select the resistor value to be used in the test and to estimate its duration. Assuming the resistor values from those available in the laboratory and knowing the measured value of the battery voltage, the corresponding maximum currents has been calculated using the first Ohm's law:

$$I = \frac{V}{R}$$

Once the maximum current values for each resistive load have been obtained, knowing that the nominal capacity of the battery is $5.2\ Ah$, the C-rate has been evaluated:

$$C = \frac{I}{5.2\ Ah}$$

On the other hand, the discharge time has been estimated using the formula below:

$$t_{discharge} = \frac{1}{C}$$

Moreover, the selection of the resistive load for both the sun simulation test and the EPS integration test has been made under the assumption that the resistive load should simulate the most power demanding operative mode, which is the commissioning mode, as reported in the power budget in Section 2.4.2. Some calculations have been performed to derive the resistor value that simulates the maximum power demand, assuming that the load port of the EPS board is used, which allows the resistive load to be supplied with a voltage of approximately $12\ V$. The following expression is considered for calculating the simulated resistance of each subsystem of the CubeSat and the results are shown in the table below.

$$R = \frac{V^2}{P}$$

Table E - 1: *CubeSat resistance estimation*

Subsystem	Voltage [V]	Power [W]	Resistance [Ω]
ADCS	12	1.31	109.92
Payload	12	5.15	27.96
ComSys	12	1.44	100
OBC	12	0.33	436.36
EPS	12	6	24
TOTAL		14.23	698.25

Resistors of the obtained value available in the STARlab had a low power dissipation value, so it has been chosen to calculate the simulated resistance values for the different supply lines of the EPS board.

Table E - 2: *CubeSat resistance estimation for different supply lines*

Subsystem	**R [Ω] @ 3.3 V**	**R [Ω] @ 5 V**	**R [Ω] @ 9 V**
ADCS	8.31	19.08	61.83
Payload	2.11	4.85	15.73
ComSys	7.56	100	56.25
OBC	33	7576	245.45
EPS	1.82	417	13.50
TOTAL	**52.81**	**203.86**	**392,76**

Therefore, the closest possible resistor has been found for the worst case, which is at $3.3\ V$ supply line. Hence, a 67 Ω resistor has been chosen, which in the sun simulation test and the EPS integration test has been connected to the supply line at approximately $12\ V$, thus representing the worst possible case.

References

[1] NASA, "Small Spacecraft Technology State of the Art Report," 2021. [Online]. Available: https://www.nasa.gov/smallsat-institute/sst-soa.

[2] Cal Poly CubeSat Laboratory, "PolySat," [Online]. Available: https://www.polysat.org/.

[3] "CubeSat Design Specification Rev. 14.1," California Polytechnic State University, San Luis Obispo, 2022. [Online]. Available: https://www.cubesat.org/.

[4] S. Corpino, N. Viola, F. Stesina and S. Chiesa, "Design and development of the e-st@r CubeSat," in *60th International Astronautical Congress*, Daejeon, Republic of Korea, 2009.

[5] G. Obiols-Rabasa, S. Corpino, R. Mozzillo and F. Stesina, "Lessons learned of a systematic approach for the e-st@r-II CubeSat environmental test campaign," in *66th International Astronautical Congress*, Jerusalem, Israel, 2015.

[6] L. Iossa, M. Centrella, E. La Bella and others, “3U CubeSat mission to assess vegetation hydration status and hydrological instability risk,” in *73rd International Astronautical Congress*, Paris, France, 2022.

[7] SRE-PA & D-TEC staff, "Margin philosophy for science assessment studies," European Space Research and Technology Centre, 2012. [Online]. Available: https://sci.esa.int/documents/34375/36249/1567260131067-Margin_philosophy_for_science_assessment_studies_1.3.pdf.

[8] J. R. Wertz and W. J. Larson, Space Mission Analysis and Design, 3rd ed., El Segundo, California: Microcosm Press, 1999.

[9] CESI, “Space Solar Cells,” [Online]. Available: https://www.cesi.it/space-solar-cells/.

[10] AAC Clyde Space, “Space product & components,” [Online]. Available: https://www.aac-clyde.space/what-we-do/space-products-components.

[11] AZUR SPACE, “Space solar cells,” [Online]. Available: https://www.azurspace.com/index.php/en/products/products-space/space-solar-cells.

[12] Rocket Lab, “Space solar cells/cics,” [Online]. Available: https://www.rocketlabusa.com/space-systems/solar/space-solar-cellscics/.

[13] Spectrolab, “Space Cells & CICs,” [Online]. Available: https://www.spectrolab.com/photovoltaics.html#cells_cics.

[14] DHV Technology, “Products,” [Online]. Available: https://dhvtechnology.com/products.

[15] ISISPACE, “Small satellite solar panels,” [Online]. Available: https://www.isispace.nl/product/isis-cubesat-solar-panels/.

[16] EnduroSat, “CubeSat Modules,” [Online]. Available: https://www.endurosat.com/products/.

[17] GomSpace, “Power Systems,” [Online]. Available: https://gomspace.com/shop/subsystems/power/default.aspx.

[18] Ibeos, “Standard Products,” [Online]. Available: https://www.ibeos.com/standard-products.

[19] Saft, “Space products & solutions,” [Online]. Available: https://www.saftbatteries.com/market-sectors/aerospace-defense/space.

[20] CubeSatShop, “EXA BA0x High Energy Density Battery Array,” [Online]. Available: https://www.cubesatshop.com/product/ba0x-high-energy-density-battery-array/.

[21] NGR srl, “Batteries,” [Online]. Available: http://www.nrgbatteries.com/en/category/batteries/.

[22] NanoAvionics, “CubeSat components,” [Online]. Available: https://nanoavionics.com/cubesat-components/.

[23] ECSS-E-ST-20-20C, "Electrical design and interface requirements for power supply," ESA-ESTEC Requirements & Standards Division, 2016. [Online]. Available: https://ecss.nl/standard/ecss-e-st-20-20c-space-engineering-electrical-design-and-interface-requirements-for-power-supply-15-april-2016-2/.

[24] Erik Kulu, "Nanosats Database," [Online]. Available: www.nanosats.eu.

Acknowledgement

First and foremost, I would like to thank my supervisors, Professor Fabrizio Stesina and Professor Sabrina Corpino, who made me passionate about the CubeSat world, since their Space Mission Analysis and Desing course until the experience I had in the CubeSat Team.

A thank you from the bottom of my heart goes to the love of my life, Dario, who has been my greatest daily support, always encouraging me at times when I thought I could not make it.

A thank you from the bottom of my soul goes to Marianna, who has been a constant in this journey of uncertainty. Thank you for teaching me what it means to have a sister, how to be more attentive and accurate and to take care of me.

A special thanks goes to my brother Massimiliano, who has taught me to be aware of everything around me and to awaken me from the dream world I was living in until recently.

I would like to thank my lifelong friend, Gianluca, with whom we have grown together in so many aspects of life and who has helped me with his precious advices in many life situations, making me the conscious person I am today.

Many thanks are also due to my parents, who supported me on this journey, and to my brother Roberto, who taught me to be a resolute person and never give up.

I would also like to thank all the people who have been close to me in many life moments, all my friends, the CubeSat Team guys, and all the people I have met, for long or short periods of life, because all of you have left me something, which has made me the person I am today.